



final report

Project code: B.CCH.1068
Prepared by: Ian Johnson
IMJ Consultants
Date published: August 2012

PUBLISHED BY
Meat & Livestock Australia Limited
Locked Bag 991
NORTH SYDNEY NSW 2059

Managing carbon in Livestock systems: modelling greenhouse gas emissions from Australian pasture systems

Meat & Livestock Australia acknowledges the matching funds provided by the Australian Government to support the research and development detailed in this publication.

This publication is published by Meat & Livestock Australia Limited ABN 39 081 678 364 (MLA). Care is taken to ensure the accuracy of the information contained in this publication. However MLA cannot accept responsibility for the accuracy or completeness of the information or opinions contained in the publication. You should make your own enquiries before making decisions concerning your interests. Reproduction in whole or in part of this publication is prohibited without prior written consent of MLA.

Abstract

The SGS Pasture Model is a mechanistic biophysical pasture simulation models, that has been widely used to address a range of research questions in Australia. The model includes pasture growth and utilization by grazing animals, animal metabolism and growth, water and nutrient dynamics, and options for pasture management, and fertilizer application. To date, the model has been applied primarily in southern Australia, and the present project has extended the scope of the model to include northern Australia. The primary focus of the project has been to assess the potential for the model to be used as an integrated plant, water, nutrient, and animal, tool for assessing carbon dynamics in Australian livestock pasture systems, and understanding how they are influenced by management. Details of model developments are presented as well as a range of simulations for 12 sites across Australia for all states and territories (except the ACT). The biophysical structure of the model, coupled with its easy-to-use interface, makes it an ideal tool for researchers seeking strategies for greenhouse gas mitigation.

Executive Summary

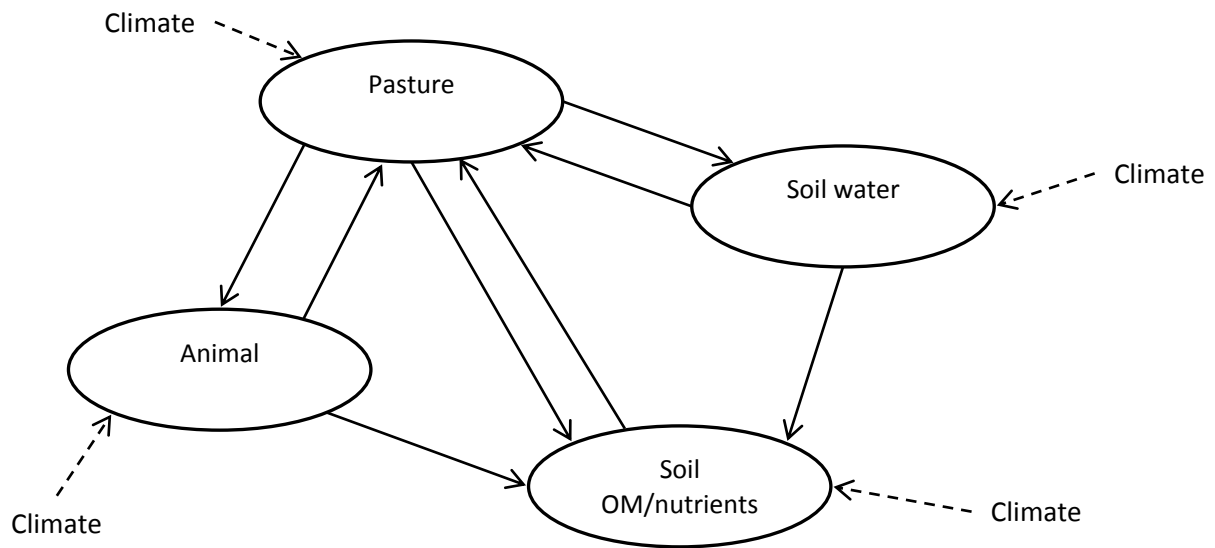
This report for project B.CCH.1068 discusses the potential for using the SGS Pasture Model to simulate greenhouse gas (GHG) emissions from Australian pastures. The report discusses:

- The outputs and simulations for 12 representative sites across Australia demonstrating the model application for northern and southern climatic regions.
- The key features of the analysis include:
 - native and improved pastures
 - sheep and beef systems
 - all states and the Northern Territory
 - the impact of fire where relevant
 - the role of trees and shrubs, where relevant, and their potential for mitigation
- A plan for future application of the model as a tool for analysing whole system CO₂e dynamics in Australian livestock pasture systems.

The aim of the work was to demonstrate the potential of the SGS Pasture Model for use in the study of GHG dynamics and possible mitigation strategies for grazing systems around Australia. The modelling work uses the SGS Pasture Model, a biophysical mechanistic pasture simulation model which includes plants, animals, soil water and nutrient dynamics, and associated GHG dynamics. Each component of the model is described at a similar level of complexity as is necessary to model greenhouse gas dynamics. The biophysical approach provides more insight into the behaviour of the system than purely empirical models and a more balanced and comprehensive approach to interactions between processes than models that only focus on a single component. The underlying structure is mathematical and therefore transparent. All model parameters can be examined and altered by users.

One of the main challenges facing the long-term analysis of GHG dynamics is that there is little available long-term experimental data for soil carbon dynamics, methane and nitrous oxide emissions. Because the SGS Pasture Model is a process based model of the plant, animal, soil water, soil organic matter, and nutrient dynamics, the variation in factors such as growth rate, soil carbon, and the overall GHG emissions are emergent properties.

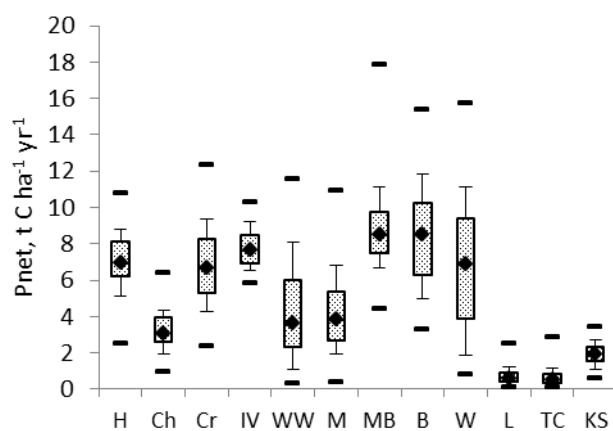
The model structure is illustrated in the figure:

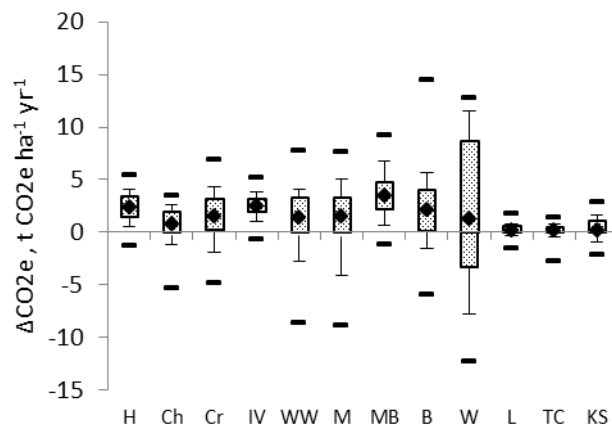


Overview of the model structure. The dashed lines indicate climatic inputs and the solid lines interactions between individual components.

Simulations are presented for 12 varying locations around Australia, including all states and the NT. Sheep and beef enterprises, as well as a range of pasture species compositions, are considered. The simulations include, where appropriate, fire, the impact of trees on pasture productivity, and discussion of grazing and fertilizer management on GHG dynamics.

A key feature of the analysis is to look at long-term variation in productivity and the associated GHG dynamics. As an example, the figure below shows the net carbon flux into the pasture system (through photosynthesis) and the associated GHG emissions in CO₂ equivalents units, which includes soil carbon dynamics, stock methane emissions, soil nitrate production through denitrification, as well as methane and nitrous oxide emissions from fire. This large variation in carbon fluxes demonstrates the importance of conducting long-term analyses in order to capture the effect of climate fluctuations on GHG dynamics.





Annual carbon fixed through photosynthesis, P_{net} , left. Annual CO_2e emission, ΔC_{soil} , right for sites as indicated by their first letter(s). Vic: Hamilton, Chiltern. Tas: Cressy. SA: Inman Valley. NSW: Wagga Wagga, Moree. WA: Mt Barker, Badgingarra. Qld: Woodstock, Longreach. NT: Tennant Creek, Kidman Springs. The symbols are the median, the box is the 25 to 75 percentile range (and so includes half of the data), the whiskers are the 10 and 90 percentiles, and the dashes the minimum and maximum.

The analysis in this report demonstrates the potential for using the SGS Pasture Model at all grazing locations in Australia to study GHG dynamics and explore possible mitigation strategies. Recent developments to the model have been presented, including the treatment of the impacts of fire in northern pastures. The C and N dynamics in pastures are complex, with interactions throughout the system. Since it is a mechanistic model for plant, soil water, soil nutrient and animal processes, and most model parameters have a direct biophysical interpretation, the model can be applied at a wide variety of locations with parameter values selected according to understanding of the underlying system. The model has an intuitive interface and so is directly accessible to users with little or no modelling skills. The developments in this project ensure that it will be of benefit to anyone working in the field of greenhouse gas mitigation in Australian pasture systems.

Contents

1	Introduction	8
2	Background	10
3	Simulations.....	11
3.1	Core simulations	12
3.2	Influence of soil type at kidman springs.....	18
3.3	Impact of fire on GHG emissions.....	18
3.4	Impact of trees on pasture production & GHG emissions.....	19
3.5	Role of management on pasture production.....	20
3.6	Influence of fertilizer application on pasture production and GHG emissions	21
4	Discussion.....	22
5	References	24
6	Acknowledgements	25
7	Appendix.....	25
7.1	Appendix 1: Model Structure	25
7.1.1	Pasture growth.....	26
7.1.2	Soil Hydrology and evapotranspiration.....	27
7.1.3	Soil organic matter and nutrient dynamics	28
7.1.4	Soil methane oxidation.....	32
7.1.5	Fire	33
7.1.6	Impact of trees on pasture growth	35
7.1.7	Animal intake, metabolism, growth and nutrient returns	36
7.2	Appendix 2 GHG dynamics in pasture systems	36
7.3	Site characteristics.....	37
7.3.1	Hamilton Vic.....	38
7.3.2	Chiltern, Vic.....	39
7.3.3	Cressy, Tas	40
7.3.4	Inman Valley, SA	41
7.3.5	Wagga Wagga, NSW.....	42
7.3.6	Moree, NSW.....	42
7.3.7	Mt Barker, WA.....	43
7.3.8	Badgingarra, WA.....	44

7.3.9	Woodstock, QLD	44
7.3.10	Longreach, QLD	45
7.3.11	Kidman Springs, NT	46

1 Introduction

This report for project B.CCH.1068 discusses the potential for using the SGS Pasture Model to simulate greenhouse gas (GHG) emissions from Australian pastures. The scope of the project is more general than the title indicates, as it covers the whole of Australia. The report discusses:

- The outputs and simulations for 12 representative sites across Australia demonstrating the model application for northern and southern climatic regions.
- The key features of the analysis include:
 - native and improved pastures
 - sheep and beef systems
 - all states and the Northern Territory
 - the impact of fire where relevant
 - the role of trees and shrubs, where relevant, and their potential for mitigation
- A plan for future application of the model as a tool for analysing whole system CO₂e dynamics in Australian livestock pasture systems.

The modelling work uses the SGS Pasture Model (Johnson *et al.*, 2003), a biophysical mechanistic pasture simulation model which includes plants, animals, soil water and nutrient dynamics, and associated GHG dynamics. Each component of the model is described at a similar level of complexity as is necessary to model greenhouse gas dynamics. The biophysical approach provides more insight into the behaviour of the system than purely empirical models and a more balanced and comprehensive approach to interactions between processes than models that only focus on a single component. The underlying structure is mathematical and therefore transparent. All model parameters can be examined and altered by users.

One of the main challenges facing the long-term analysis of GHG dynamics is that there is little available long-term experimental data for soil carbon dynamics, methane and nitrous oxide emissions. Because the SGS Pasture Model is a process based model of the plant, animal, soil water, soil organic matter, and nutrient dynamics, the variation in factors such as growth rate, soil carbon, and the overall GHG emissions are emergent properties.

The elements of GHG dynamics in pastures are:

- photosynthesis
- the dynamics of the transfer of carbon from litter, dung and plant root senescence into the soil carbon pool
- soil organic matter dynamics and turnover, including soil carbon respiration
- animal intake and its effect on pasture production as well as dung and urine inputs
- methane emissions from animals and fire
- nitrous oxide emissions from soil denitrification and fire

These processes are all inter-related. For example, greater plant growth may lead to increased fluxes of carbon into the system, while soils with low soil organic matter may be nutrient deficient and so reduce plant growth. Similarly, plant availability influences animal intake, growth and metabolism and so affects methane emissions as well as nutrient returns to the soil and the subsequent impact on plant growth and soil denitrification.

A fundamental objective in the development of the SGS Pasture Model has been to ensure that model parameters have an underlying biophysical interpretation and that the parameter values defining biophysical processes are generic and not specific to individual sites.

For example, with a pasture species such as phalaris, the same set of physiological parameters can be applied at any location and, though different varieties may have different physiological characteristics, key parameters can be modified with knowledge of the characteristics of each variety.

This approach has been applied, for example, by Cullen *et al.* (2008) who, with the knowledge that later varieties had better growth at low temperatures, were able to model both old and more recent varieties of perennial ryegrass.

A key aspect of soil carbon dynamics is the flux of carbon into the system. Consider an example where input to the soil carbon pool is estimated and then the rate of carbon decay adjusted so that net soil carbon is in agreement with current (static) measurements. It would seem to 'validate' the model. However, if that input was unknowingly underestimated, it would still be possible, by reducing the rate of decay of the soil carbon, that again the net soil carbon is in agreement with the current measurements. In this latter case, the 'right' answers have been obtained for the 'wrong' reasons.

Testing and evaluating large-scale biophysical models has been discussed extensively in the literature (e.g. Oreskes *et al.*, 1994). I also wrote about this in a keynote presentation at the recent MODSIM conference (Johnson, 2011). Oreskes *et al.*'s argument is that it is never possible to prove the truth of a model that describes an *open* system – that is, a system where neither the data nor the theory capture all of the factors affecting the underlying system behaviour. In light of these studies, I prefer to use the term *testing and evaluating* rather than *validation*. The simulations presented here can be assessed through their general characteristics, such as pasture production, soil carbon dynamics, and GHG emissions, and their variation through time at different sites.

The SGS Pasture Model has been developed primarily with funding from MLA (and has the same underlying biophysical core as DairyMod, Johnson *et al.*, 2008, funded by Dairy Australia.). The Model has been applied extensively in the published literature to a variety of research questions, which include comparisons with experimental data from many geographical locations for a range of pasture species, as well as addressing important questions such as climate variability, drought, business risk, and the impacts of climate change. The biophysical structure of the model means it is well suited to be developed to explore issues such as new management strategies or plant characteristics, as well as the environmental impacts of possible future climate change scenarios. The present project adds the analysis of GHG dynamics in pasture systems and includes locations in northern Australia. Simulations are presented below for 12 sites across Australia, and represent all states and territories with the exception of the ACT. The climate data used for simulations are taken from the SILO database (Jeffrey *et al.*, 2001) for the period 1901 to 2011 inclusive. These sites and simulations are discussed in more detail later, but first, aspects of the model development relevant to the current project are considered.

2 Background

The model is a daily time-step model that includes pasture growth and utilization by grazing animals, animal metabolism and growth, water and nutrient dynamics, and options for pasture management, and fertilizer application. The climate inputs for the model are rainfall, maximum and minimum temperature, solar radiation, vapour pressure, as well as site latitude and elevation. A key characteristic of the model is the interaction between the individual modules, as illustrated in Fig. 1. An outline of the model structure is presented in Appendix 1. The main developments of the model within the current project have focused on soil carbon dynamics and fire and so the implementation of these processes are described in detail in Appendix 1. Soil methane dynamics and the implementation of the impact of trees are also discussed.

Tree growth dynamics are important in the consideration of GHG mitigation strategies. Well-established models, widely used in Australia, such as the FullCam model, are available for such studies. As a result of discussions at the MLA workshop in Brisbane (May, 2012), the present model has not been adapted to include a detailed tree growth model since it is preferable to use these other models. However, trees are a part of many pasture systems, particularly in the NT and Qld, and so the impact of trees on pasture growth has been incorporated, as described in Appendix 1.

Shrubs are significant in northern pasture systems, and have been incorporated in the model. In the simulation for Woodstock, Qld, the shrub *stylo* is included. It is available for grazing and also, being a legume, is a source of N fixation.

The model includes all of the fluxes of carbon and nitrogen that are required to do a complete GHG analysis for pasture systems, and the details of these calculations are presented in Appendix 2.

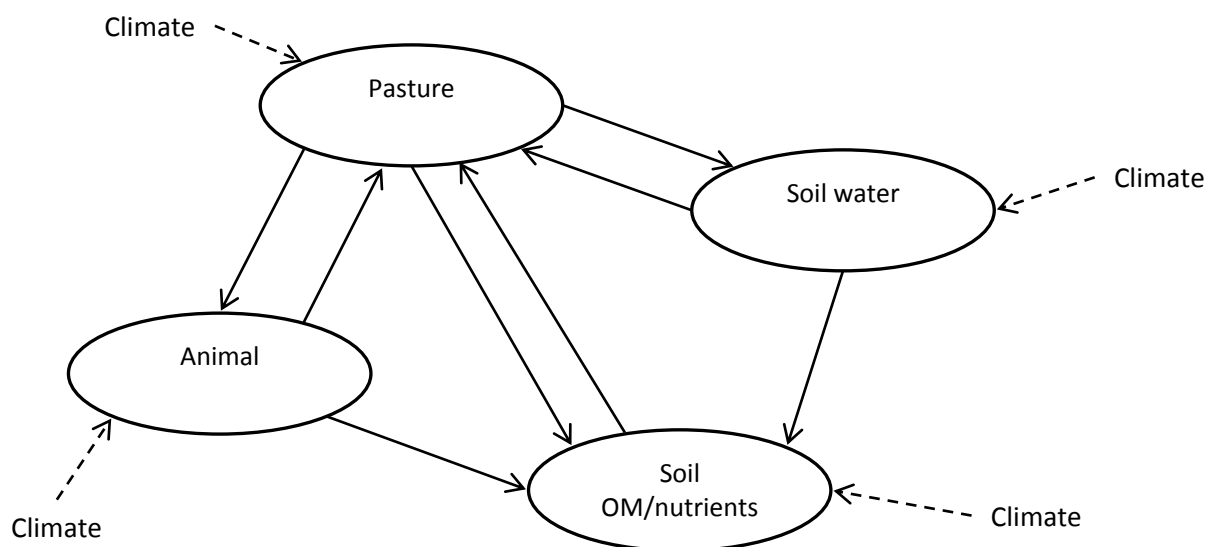


Figure 1. Overview of the model structure. The dashed lines indicate climatic inputs and the solid lines interactions between individual components.

As well as having a sound underlying biophysical mechanistic structure, the model has also been designed to be accessible to researchers.

To this end, two important criteria have been applied: first, that all parameters in the model should have a direct biophysical interpretation; and second, that the model interface has been designed to allow users to work effectively with the model without requiring any programming skills.

The model can be downloaded from <http://www.imj.com.au/consultancy/sqs5/sqs5.html>. A license key is required to run the model and this can be obtained from Ian Johnson via email (ian@imj.com.au). The model includes options for set-stocked and rotational grazing with up to 30 paddocks. If more paddocks are required, this it would be relatively straightforward to adapt the code accordingly.

3 Simulations

Sites and simulation details are presented in Table 2. These have been selected to represent a range of climatic characteristics around Australia. There are 6 native pasture systems and 6 improved. The native pasture systems in southern Australia use generic C₃ and C₄ species, representing a mixed species sward. For the Woodstock simulation (Qld), a medium quality generic C₄ species is used. This differs from the species used for the southern simulations in that a lower proportion of new growth is partitioned to the leaves. Similarly, the Longreach (Qld) and NT simulations use a low quality generic C₄ species with lower growth partitioned to the leaves and thicker leaves. All parameters can be accessed on the model interface. All of the southern improved pastures include a clover species, which can be taken to represent either white clover or sub-clover. The Woodstock simulation includes *stylo*, which is a shrub legume.

Table 2. Sites and simulations. Longitude and latitude are given in decimal units. Mean annual rainfall, mm yr⁻¹, is for the period 1901 to 2011 inclusive from the SILO database (Jeffrey *et al*, 2001).. Stock numbers apply when the paddock is being grazed. If fire is ticked then the paddock burns on 1 Sept every 5 years. See text for more detail.

Location, abbreviation	lat, decimal	long	Mean rain mm yr ⁻¹	Pasture	Stock	Fire
Vic						
Hamilton	H	-37.75, 142	676	Phalaris, clover	30 wethers ha ⁻¹	
Chiltern	Ch	-36.15, 146.6	674	Native C3, C4	10 wethers ha ⁻¹	
Tas						
Cressy	Cr	-41.7, 147.1	627	P. ryegrass, clover	20 wethers ha ⁻¹	
SA						
Inman Valley	IV	-35.5, 138.45	875	Phalaris, clover	30 wethers ha ⁻¹	
NSW						
Wagga Wagga	WW	-35.1, 147.4	530	Phalaris, clover	20 wethers ha ⁻¹	
Moree	M	-29.45, 149.9	577	Native C3, C4	8 wethers ha ⁻¹	
WA						
Mt Barker	MB	-34.65,	708	Kikuyu, clover	30 wethers ha ⁻¹	

		117.65			¹	
Badgingarra	B	-30.35, 115.55	567	Rhodes grass, clover	15 wethers ha ⁻¹	
Qld						
Woodstock	W	-19.6, 146.85	908	Rhodes grass, stylo	1 steer ha ⁻¹	✓
Longreach	L	-23.45, 144.25	425	Native C4	10 steers km ⁻²	✓
NT						
Tennant Creek	TC	-19.65, 134.2	390	Native C4	10 steers km ⁻²	✓
Kidman Springs	KS	-16.1, 130.95	705	Native C4	10 steers km ⁻²	✓

3.1 Core simulations

To demonstrate the general characteristics of the long-term site responses, a set of simulations for each site are first considered. Stock management tends to be more intense in southern systems due to the size of the grazing enterprises. Consequently, for the sheep simulations, stock are removed from the paddock if the dry weight (d.wt) falls below 1 t ha⁻¹ and are returned when it reaches 2 t ha⁻¹. For these simulations, animal growth is not included, and a simple grazing animal that consumes pasture and returns dung and urine is represented. The grazing animal is always at its normal mature weight and no product removal was considered in these simulations. Therefore, animal daily energy requirement remains constant and, when combined with the energy density of the pasture, defines the daily animal pasture intake requirement. Any reduction in intake is due to lack of available pasture. Intake by grazing animals influences pasture growth through its effect on green dry matter and canopy photosynthesis. Consequently, the animal numbers in Table 2 for these locations are quite high compared with normal stocking rates. However, it must be emphasised that the animals were not on the paddock for the full duration of the simulations.

For Qld and NT pasture systems, stock management is less intense due to the extensive nature of the grazing enterprise. For these systems, stock numbers are generally conservative to accommodate years when growth is low. For the steer simulations, the paddocks remain set-stocked throughout the simulation period and animal growth is included. There is no supplementary feeding.

Note that other management systems are considered later, including animal growth and supplementary feeding.

One of the challenges facing the analysis of GHG dynamics in pastures is the large variability in climatic conditions, particularly rainfall, that affect pasture production. This variability is clearly apparent from the illustrations in Appendix 3 where summaries of rainfall and temperature are presented for each site. Here it can be seen that the chosen locations cover the spread of climatic conditions in Australia from cool temperate to tropical and winter or summer dominant rainfall. Regardless of the location, it is clear that the one consistent characteristic of rainfall patterns is their considerable variability. This results in large degrees of variation in pasture production and carbon dynamics.

The emphasis of the present analysis is to look at long-term carbon dynamics based on nutrient cycling alone. Thus, no fertilizer nitrogen applications were included. This means that the only N inputs were from N fixation by clover, if present, and atmospheric deposition.

It was assumed that atmospheric N inputs were $3 \text{ kg N ha}^{-1} \text{ yr}^{-1}$; although this is a small value, it is sufficient to offset N losses in the native systems while, for the improved systems, N inputs are dominated by N fixation.

The same set of soil hydrology and nutrient dynamics parameters were used for all simulations. While hydrology parameters can vary from paddock to paddock, there are no general patterns for different locations. The possible exception to this is the high incidence of sandy soils in WA and it is straightforward to modify these parameters in the model as required. Although soil organic matter (SOM) dynamics parameters are the same for all simulations, as will be seen, the actual SOM content varies substantially in response to environmental conditions. In general, for regions where growth is high, carbon inputs to the soil are also high which results in greater SOM. However, SOM dynamics are affected by soil water status and temperature, and so SOM tends to be quite variable for different locations and pasture systems. See Appendix 1 for details on the hydrology and SOM dynamics in the model.

The initial amount, and nitrogen composition, of the SOM can have a marked impact on simulation results. These are difficult to prescribe accurately and so one of two common starting points are used for all simulations. The simulations are then run 3 times without re-initializing the system state variables, and the output from the third of these is used for analysis. This means that the simulations are run for 222 years (using 111 years of climate data twice) before a third run of 111 years for analysis. This strategy is referred to as ‘spinning-up’ the model. These initial soil carbon distributions, for low and medium SOM, are shown in Fig. 2, which is equivalent to 41 and 28 t C ha^{-1} respectively in the top 30 cm. The initial C:N ratios for the fast and slow pools are 12 for the medium SOM and 18 for the low SOM. In both cases the C:N ratio of the inert pool is 30. For all sites, the simulations reached a dynamic equilibrium where, in subsequent simulations, the SOM pools were in long-term equilibrium, indicating that the original choice of soil organic matter content and C:N ratio was not influencing the results. However, as will be seen, there were short-term fluctuations in the SOM in response to climate variation. Also, while the C:N ratio of the inert pool did not change, for the fast and slow turnover pools it responded dynamically. The native pasture simulations were initialized with the lower SOM while the remainder had the medium SOM. It should be noted that if the simulations are allowed to run for long enough the choice of initial conditions has no influence. These different starting values were chosen to reduce the ‘spin-up’ time required.

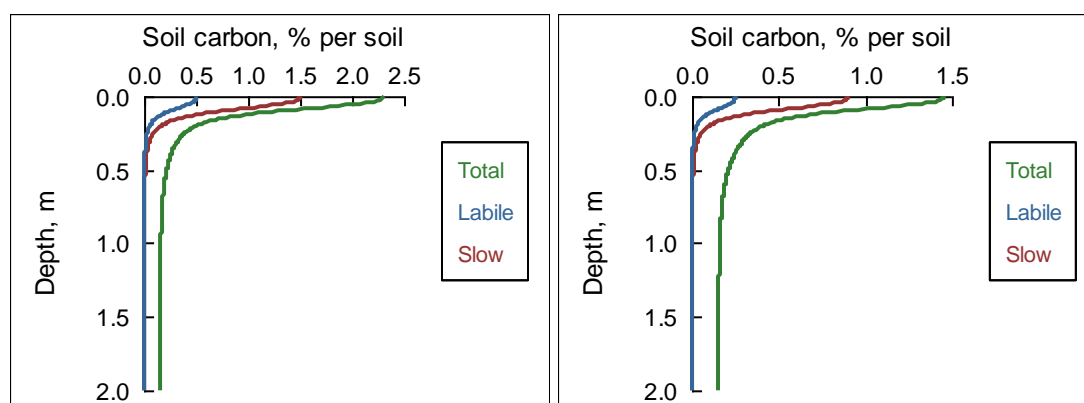


Figure 2. Initial SOM distribution in the soil for the medium (left) and low (right) SOM soils.

The overall carbon and GHG dynamics for each of the sites in Table 2 are now considered. Recall that all simulations were close to dynamic equilibrium, so that there was little change in the net soil carbon over the simulation period of 111 years.

However, fluctuations between years do occur. Figure 3 shows the annual carbon fixed at each site, P_{net} , and the corresponding change in soil carbon, ΔC_{soil} , along with their variability. The potential for large fluctuations in system dynamics is clearly apparent in both P_{net} and ΔC_{soil} .

While the soil carbon change was negligible over the 111 year simulation period, fluctuations of close to 4 t C ha^{-1} (in the top 30 cm) occurred. All sites showed substantial variability in both P_{net} and ΔC_{soil} , although carbon fixed (P_{net}) was lowest at Longreach, Tennant Creek and Kidman Springs, as might be expected due to the generally harsher growth conditions.

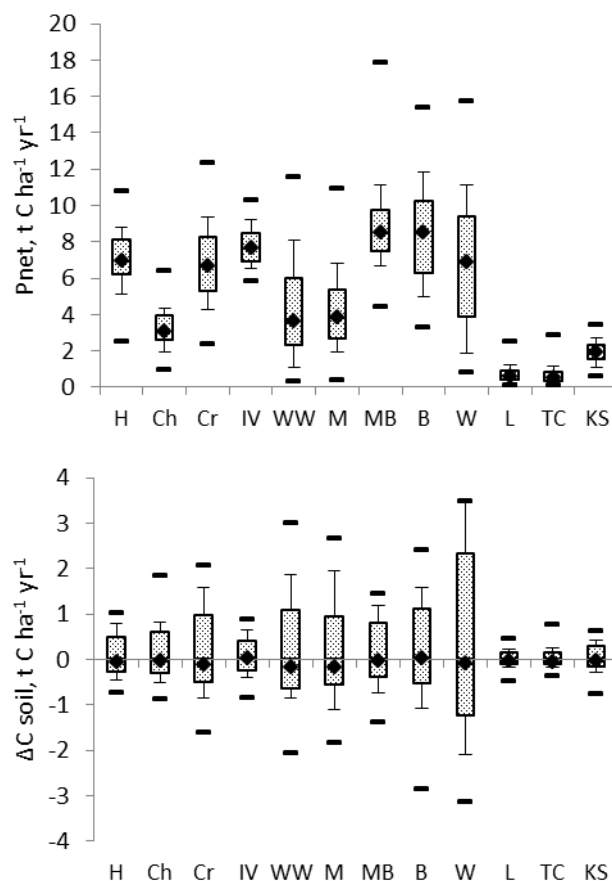


Figure 3. P_{net} , left, ΔC_{soil} , right for each site as indicated by their first letter(s) (see Table 2). Note that ΔC_{soil} is presented for the top 30 cm of the soil profile. The symbols are the median, the box is the 25 to 75 percentile range (and so includes half of the data), the whiskers are the 10 and 90 percentiles, and the dashes the minimum and maximum.

The potential to store carbon in soils is an important aspect of GHG mitigation strategies. These simulations do not consider changes in management strategies that might lead to greater soil carbon storage, but focus on long-term dynamic equilibrium – that is, where the soil carbon does not vary significantly over the 111 year simulation period in spite of shorter term fluctuations as shown in Fig. 3. The soil carbon mass to 30 cm, along with its C:N ratio is shown for each site in Fig. 4. It can be seen that soil carbon is highly variable across sites, being generally greater for those with higher productivity. The C:N ratio is also subject to variability, being generally greater for regions with lower productivity and pasture quality. The C:N ratio is shown for the total SOM and also just for the fast and slow turnover pools, that is, not including the inert carbon (taken to be C:N = 30). It can be seen that inert carbon influences the total C:N ratio.

Note that all sites have the same absolute mass of inert carbon in these simulations, although the proportions differ due to the system dynamics.

One point to note is that in the simulations with fire (Woodstock, Longreach, Tennant Creek, Kidman Springs) there is an increase in the inert soil organic matter pool. This is due to the direct input from the burnt material. In the model, this inert material (by definition) does not decay so that if the model were run for thousands of years there would be a slow but continual increase in the inert soil carbon. However, the model is intended for simulations over a few hundred years and so this is not an important issue. It could be readily addressed if necessary.

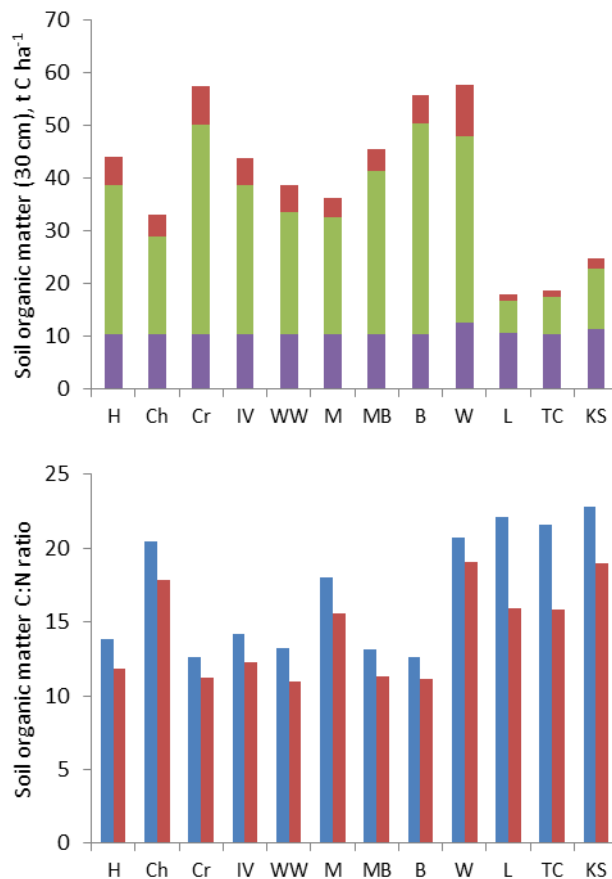


Figure 4. Left: soil organic matter in the top 30 cm of the soil profile at the end of the simulations. The lower bar is inert carbon (set to the same value for each site), middle box is slow turnover carbon, and the upper box is fast turnover carbon. Right: corresponding C:N ratio of the total soil organic matter: the blue bar includes the inert SOM component, and the red bar is only the fast and slow turnover pools. Sites are indicated by their first letter(s).

Soil carbon dynamics are influenced by the flux of carbon into soil organic matter and soil organic matter decay. As discussed in Appendix 1, the decay rates depend on soil water content and temperature and, in addition, the decay rate of the fast turnover pool is affected by the quality of senescent material. Consequently, while the same model parameters have been used at all sites, the decay rates differ. To illustrate this, average half-lives for the fast, h_F yr and slow, h_S yr, turnover pools are presented in Fig. 5 for each site. Half-lives are calculated by taking the annual average value of decay constants k_F and k_S , eqns (9), (10), (16), (17) in Appendix 1, converting this to yr^{-1} and using the standard equation that half-life is $\ln(2) / (\text{decay rate})$. It should be noted that the *mean residence time* is also sometimes used to characterise the decay rate of SOM pools, which is the reciprocal of the decay rate (see Appendix 1 for more

discussion). For the Qld and NT simulations, half-lives are greatest (that is, decay rates are lowest) for the Longreach and Tennant Creek simulations, due to the drier conditions.

The lower half-lives at Kidman Springs and Woodstock are a result of higher summer rainfall that occurs in those regions. For the southern simulations, half-lives vary again due to differences in climatic conditions. It is interesting to note the contrast between the Wagga Wagga and Moree simulations where it can be seen that for Wagga Wagga, h_F is lower while h_S is higher. The difference in h_S is due to climatic conditions, with wetter summer conditions at Moree combined with warmer conditions resulting in greater decay. However, the decay of the fast pool is also affected by the quality of the senescent material and so is generally lower for poorer quality native pastures, which corresponds to a greater half-life.

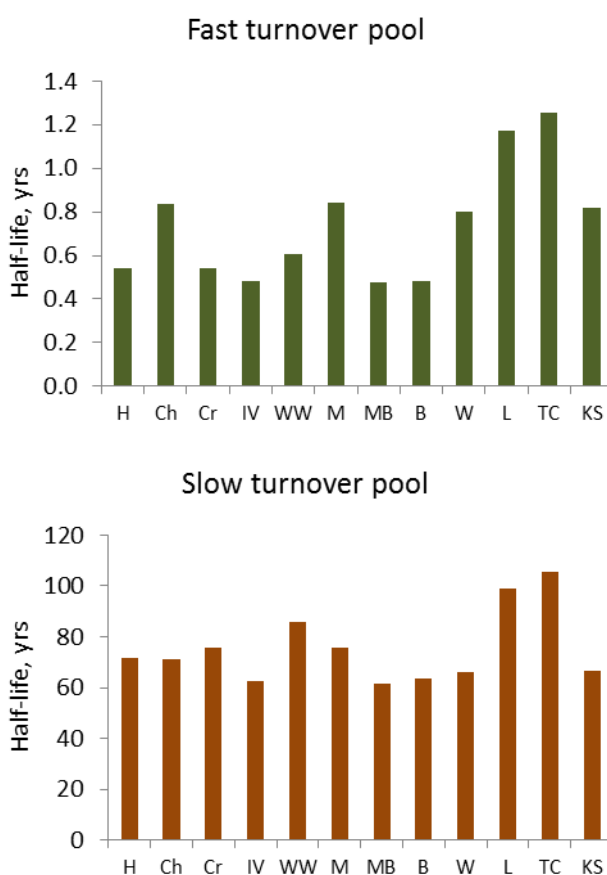


Figure 5. Half-lives (yr) for the fast (left) and slow (right) soil organic matter turnover pools, in the top 30 cm of the soil profile. Sites are indicated by their first letter(s).

While the long-term average half-lives of the soil organic matter pools are shown in Fig. 5, these, like other aspects of the system are subject to considerable variation due to fluctuating climatic conditions. As an example, h_F for Tennant Creek and h_S for Wagga Wagga are shown in Fig. 6 for each simulation year. The variation is self-evident and indicates that short-term measurements may not capture long-term trends.

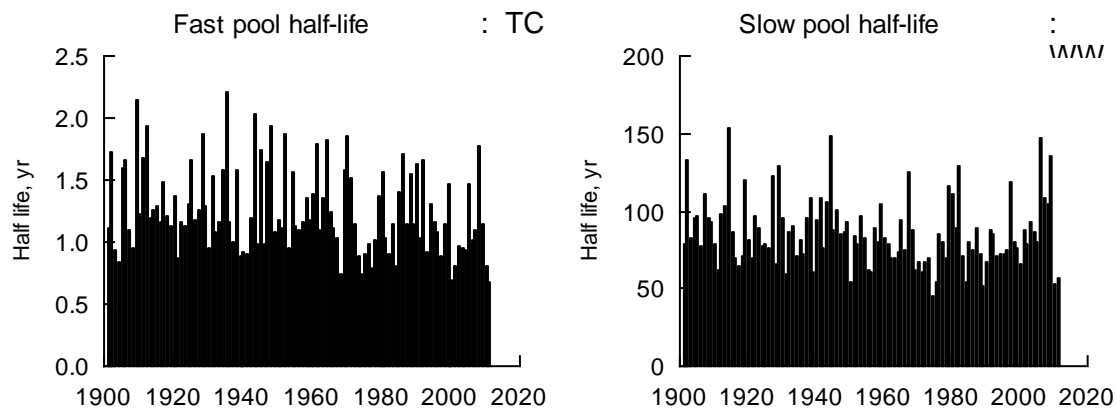


Figure 6. Half-life (yr) for the fast soil organic matter turnover pool at Tennant Creek (left) and slow soil organic matter turnover pool at Wagga Wagga (right), in the top 30 cm of the soil profile, for each year of the simulations.

Attention so far has focused on carbon, and CO₂e dynamics are now considered as defined by eqn (25) in Appendix 2. The net outgoing CO₂e, ΔCO_2e t CO₂ ha⁻¹ yr⁻¹ for each site is illustrated in Fig. 7. Overall, all sites had a long-term efflux of CO₂e, due to the relatively high conversion coefficients for CH₄ and N₂O. However, all sites did have years when there was a net influx of CO₂e to the system, due to a net accumulation of soil carbon which was sufficient to offset CH₄ and N₂O emissions. For all sites there was considerable variation in the CO₂e dynamics, indicating that short-term studies may not capture long-term variability.

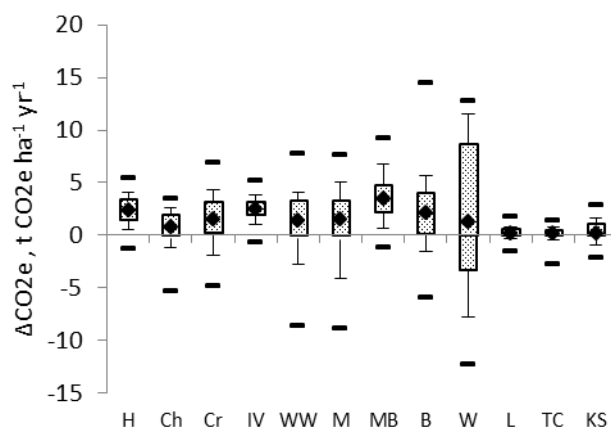


Figure 7. Net outgoing CO₂e, ΔCO_2e t ha⁻¹ yr⁻¹ for each site as indicated by their first letter(s). See Fig. 5 for graph description.

For these simulations that are in long-term dynamic equilibrium with little change in soil carbon over the 111 years of the simulation, GHG dynamics are generally dominated by CH₄ and N₂O emissions. Average values for CO₂e values for these are shown in Fig. 8 where it can be seen that CH₄ is generally greater than N₂O. Although emissions are very low for the northern extensive systems at Longreach, Tennant Creek and Kidman Springs, these values are expressed per ha and grazing enterprises are generally very large in these regions.

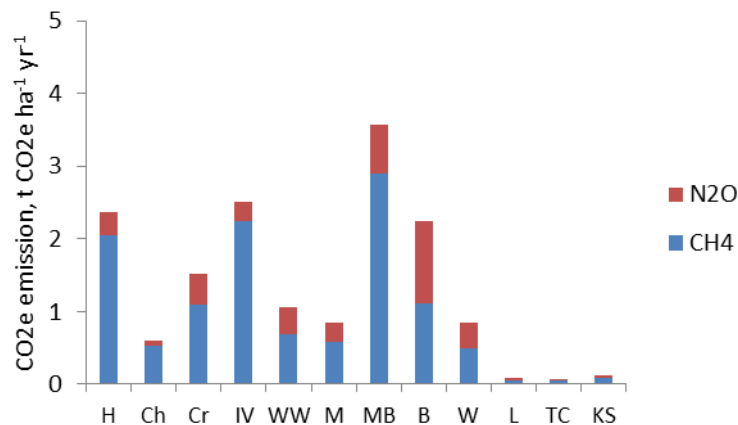


Figure 8. Net outgoing CO₂e components of CH₄ (blue) and N₂O (red) for each site as indicated by their first letter(s). Sites are indicated by their first letter(s). The illustrations presented above demonstrate that the model displays plausible behaviour for whole-system carbon and nitrogen dynamics for contrasting locations and pasture types.

3.2 Influence of soil type at kidman springs

To explore the possible impact of soil hydrology parameters, consider the Kidman Springs simulation. At the MLA modelling workshop held in Brisbane (24, 25 May, 2012), we discussed the soil carbon levels at Kidman Springs for the light and heavy soils, which were only a few km apart. Observations by Ram Dalal and Diane Allen indicated that lighter soils have higher soil carbon. This was counter to expectations that heavier soils with a greater clay content would have higher soil carbon levels. I have run the Kidman Springs simulation using the soil hydrology parameters suggested by Ram at the workshop for the light and heavy soils. Apart from the soil type, plant rooting depth has been changed so that about 80% of the roots are in the top 20cm for the heavy soil and the top 50cm for the heavy soil. Other than that, all parameters are the same for the two simulations. With these changes, the model predicts total soil carbon in the top 30 cm to be 28 and 22 t C ha⁻¹ for the light and heavy soils respectively. The observations were 28 and 20 t C ha⁻¹ respectively so the model is in close agreement with observation. Furthermore, it is encouraging that the trend from the model is consistent with observation, and that the model provides a plausible explanation that the differences in soil carbon are a result of the hydrological soil properties and their influence on pasture productivity and hence inputs to the soil organic matter pools.

3.3 Impact of fire on GHG emissions

The approach for implementing fire in the model is discussed in Appendix 1. Fire has been applied every 5 years for the Woodstock, Longreach, Tennant Creek and Kidman Springs simulations. Note that the model allows fire occurrence to be defined to occur at regular intervals or randomly. No attempt is made to predict the incidence of fire.

The CO₂e emissions for CH₄ and N₂O are shown in Fig. 9 and it can be seen that CH₄ emissions are generally greater than N₂O. The regular pattern of reduced CH₄ emission is due to the impact of fire – pasture is removed and so cannot be grazed.

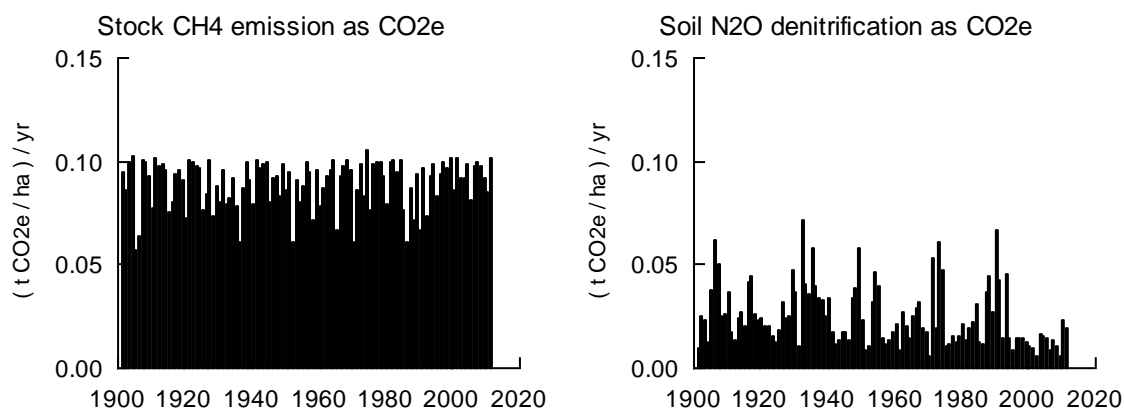


Figure 9. Annual CH₄ emissions from stock and N₂O from soil for the Kidman Springs simulation.

Emissions from fire are shown in Fig. 10 and it can be seen that they are of a similar order of magnitude to regular emissions. However, due to the frequency of fire their long-term values are lower. The annual average total CH₄ and N₂O emissions are 0.089 and 0.025 t CO₂e ha⁻¹ yr⁻¹, while the average values for fire alone are 0.006 and 0.009 t CO₂e ha⁻¹ yr⁻¹. However, if the values for fire are only considered for years when a fire occurs, the average values are now 0.139 and 0.193 t CO₂e ha⁻¹ yr⁻¹ for CH₄ and CO₂ respectively. Thus, it can be seen that emissions from fire in extensive northern pastures can exceed the magnitude of CH₄ emissions from stock and N₂O through soil denitrification in years when fires occur.

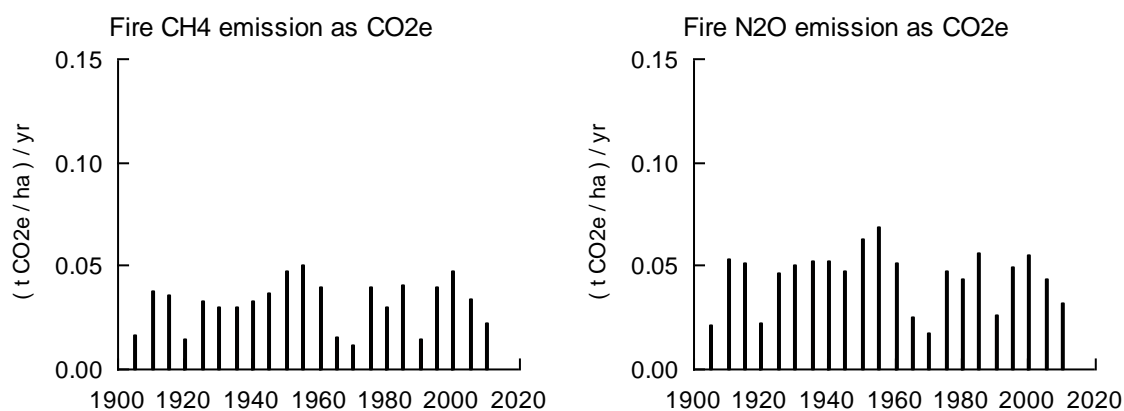


Figure 10. Annual CH₄ and N₂O emissions fire for the Kidman Springs simulation.

3.4 Impact of trees on pasture production & GHG emissions

The implementation of the effect that trees have on pasture production in the model was discussed earlier and is also discussed in Appendix 1. To illustrate impact of trees as implemented in the model, the simulation for Woodstock has been run with a tree ground cover of 20%. The general effect is to reduce carbon fixation through pasture photosynthesis. This, in turn affects animal intake and therefore methane emissions, as well as denitrification which results primarily from urine deposition. These results are presented in Table 3 where it can be seen that the reduction in net pasture photosynthesis, that is carbon flux into the system, is around 25%, and this reduction in pasture growth results in lower animal intake and therefore CO₂e emissions through stock methane production and soil denitrification.

The lower pasture production also results in lower fire emissions, although there will obviously be emissions from tree burning.

Table 3. Annual long-term average values for pasture net photosynthesis ($\text{t C ha}^{-1} \text{ yr}^{-1}$), stock methane production ($\text{t CO}_2\text{e ha}^{-1} \text{ yr}^{-1}$), soil denitrification ($\text{t CO}_2\text{e ha}^{-1} \text{ yr}^{-1}$), CH_4 and N_2O from pasture burning ($\text{t CO}_2\text{e ha}^{-1} \text{ yr}^{-1}$), for the Woodstock simulation with and without trees.

	Net phys, $\text{t C ha}^{-1} \text{ yr}^{-1}$	Stock CH_4 : CO_2e $\text{t CO}_2\text{e ha}^{-1} \text{ yr}^{-1}$	Soil N_2O : CO_2e $\text{t CO}_2\text{e ha}^{-1} \text{ yr}^{-1}$	Fire CO_2e $\text{t CO}_2\text{e ha}^{-1} \text{ yr}^{-1}$
No trees	6.79	0.487	0.361	0.042
With trees	5.10	0.442	0.275	0.033

3.5 Role of management on pasture production

Pasture management has a direct influence on pasture productivity and animal intake. The model provides for a range of management strategies and is structured to allow easy incorporation of new strategies as required. To demonstrate the basic potential of the model, the simulation for Moree has been run either with set stocking or a simple 4 paddock rotation with the animals on each paddock for 2 weeks. In the previous simulation described above, animal growth was not included and the paddock was de-stocked when pasture d.wt fell below 1 t ha^{-1} . For these simulations, animal growth is included and animals are fed supplementary forage if their weight falls below 40 kg and the pasture d.wt below 0.5 kg ha^{-1} . They are then returned to the paddock when the animal weight reaches 45 kg and pasture d.wt 1.5 kg ha^{-1} . This is intended to reflect a simple strategy based on both animal condition and available pasture. The stocking rate was $3 \text{ wethers ha}^{-1}$. To illustrate the impact of management, the annual intake of pasture and supplementary forage are shown in Fig. 11. It is immediately apparent that the rotational system results in greater pasture intake and less supplement requirement. The proportion of supplement in the diet was 24% for set stocked compared with 11% for the rotation. It should also be noted that much greater supplement was required in the first half of the last century which reflects the lower annual rainfall during this period.

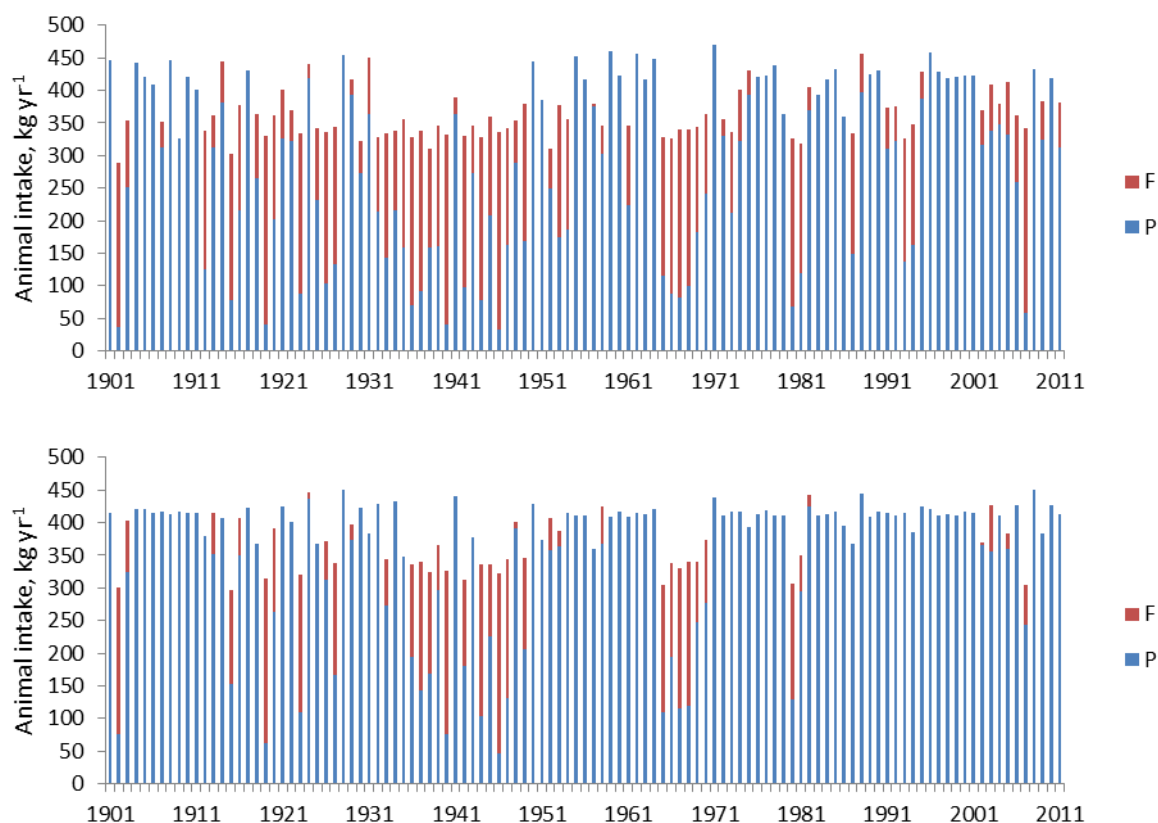


Figure 11. Annual animal intake of pasture (P) and forage supplement (F) for the Moree simulation with 3 wethers ha^{-1} . Top: set stocked. Bottom: 4 paddock rotation with paddocks grazed for 2 weeks.

While these simulations do not directly address GHG dynamics, they demonstrate that the model is robust in response to management and is well suited to analyse complex management strategies and their likely impact on GHG emissions and possible mitigation strategies.

3.6 Influence of fertilizer application on pasture production and GHG emissions

It is clear that management will influence pasture productivity which, in turn, may affect GHG dynamics. Fertilizer application is common in many pasture systems, and so the Hamilton simulation has been run with 20 kg urea nitrogen fertilizer being applied when the inorganic nitrogen concentration in the top 15 cm of the soil falls below 10 mg kg^{-1} , with a minimum time between applications of 14 days. Table 4 shows the long-term averages for the simulations with and without fertilizer N for the net carbon fixed through photosynthesis and emissions of methane and nitrous oxide. It can be seen that applying fertilizer N increases the carbon flux into the system through photosynthesis and also emissions of CH_4 and N_2O as a result of greater pasture utilization. The N_2O proportion of the total emissions increases when fertilizer N is applied, which is to be expected.

Table 3. Annual long-term average values for pasture net photosynthesis ($\text{t C ha}^{-1} \text{ yr}^{-1}$), stock methane production ($\text{t CO}_2\text{e ha}^{-1} \text{ yr}^{-1}$), soil denitrification ($\text{t CO}_2\text{e ha}^{-1} \text{ yr}^{-1}$), and the proportion of CO_2e from N_2O for the Hamilton simulation with and without fertilizer N.

	Net $\text{t C ha}^{-1} \text{ yr}^{-1}$ phys,	Stock CO_2e $\text{t CO}_2\text{e ha}^{-1} \text{ yr}^{-1}$	Soil N_2O : CO_2e $\text{t CO}_2\text{e ha}^{-1} \text{ yr}^{-1}$	N_2O percent of CO_2e
No N fertilizer	6.99	2.04	0.33	14%
N fertilizer	7.95	2.23	0.71	24%

4 Discussion

The SGS Pasture Model provides an integrated approach for the study of GHG dynamics in Australian pastures. Recent developments to the model have been presented, including the treatment of the impacts of fire in northern pastures. The C and N dynamics in pastures are complex, with interactions throughout the system. Since it is a mechanistic, process based model, and most model parameters have a direct biophysical interpretation, the model can be applied at a wide variety of locations with parameter values selected according to understanding of the underlying system.

Climate variability, in particular rainfall, leads to a high variability in pasture production and so long-term simulations are used to explore responses in GHG dynamics at a range of locations across Australia. Carbon inputs to the system from photosynthesis are either utilized directly by grazing animals or transferred to the soil organic matter. Dung and urine are also transferred to the soil organic and inorganic pools. Direct measurements of these fluxes are challenging, and the model is a powerful tool for long-term analysis, giving a direct estimate of the interactions between photosynthesis, pasture production, intake and carbon and nutrient dynamics into the soil. These processes were seen to be highly variable at all sites considered.

Soil organic matter (SOM) dynamics pose challenges due to the slow decay rates. Again, long-term simulations allow these dynamics to be explored. The model has relatively few parameters, and they all have direct biophysical interpretation. Simulations were run using the same set of parameters, with variation in SOM dynamics being due to soil water status, temperature, and quality of the inputs. By running the simulations for a lead-up period of 222 years before using a further 111 years for analysis, long-term steady state SOM occurred at all sites. However, short-term variation did occur and suggests that increases or decreases in SOM can result from climate variability alone. As well as the amount of SOM, differences occurred in the C:N ratio as a result of different pasture types and quality of senescent material. The half-lives for decay of the fast and slow turnover pools are also seen to differ across sites, due to the effects of soil water, temperature, and quality of inputs. By relating the decay rate of the fast turnover pool to quality it was possible to capture differences in fast decay without using multiple pools.

The analysis shows that the annual net efflux of CO_2e from the system was generally positive for all sites, with occasional negative values. This is due to the fact that the soil carbon is relatively stable for these long-term simulations so that CO_2e dynamics are dominated by CH_4 and N_2O emissions.

The impact of fire on CH₄ and N₂O emissions has been incorporated in the model and it can be seen that for years when fires do occur, the emissions are of similar magnitude to those from the stock and soil. Emissions from fire are directly affected by the amount of pasture burnt.

The simulations for the contrasting sites and pasture types presented here demonstrate the inherent variability in system dynamics of Australian pastures. The analysis demonstrates the potential of using the SGS Pasture Model for the study of GHG dynamics in pastures at a wide range of sites. Since it is a process based mechanistic model, all parameters have been prescribed through an understanding of the biophysics. These simulations are not definitive, but demonstrate the potential of the model to be used for analysis of GHG emissions in Australian pastures.

During this project I have had discussions with researchers around Australia, including people working with the GRASP model. In my view, the SGS Pasture Model and GRASP are entirely different but complementary in their potential to be used as part of grazing studies. The GRASP model, which has been used in a wide range of important grazing studies, is empirical in structure and so, rather than relying on a model structure based on underlying biophysical processes, it is built on an analysis of data sets. Users work with the FORTRAN computer code whereas the SGS Pasture Model has a Windows user interface that includes the potential to share biophysical parameter sets and has extensive post-simulation analysis. The models cannot be compared because of their fundamental differences. In my discussions with the GRASP researchers, I felt that we were in agreement that the models each have a role to play.

Future work with the SGS Pasture Model has the potential to explore possible mitigation strategies aimed at reducing emissions. The principal areas under discussion are:

- The incorporation of model simulations in financial analysis of carbon options. This will allow site, regional and enterprise specific factors to be included in the analysis.
- The influence of management on whole farm emissions. This will include looking at emissions intensity and how management can affect the overall carbon emissions of a farm.

The model has been used widely as a tool for researchers and, if it is to be applied to its full potential, I recommend that consideration is given to on-going development, maintenance, support and training.

The model continues to provide a unique tool for use in research projects due to its biophysical, mechanistic structure that integrates the complete system carbon and nutrient dynamics. The current project has seen the model extended to all grazing areas in Australia, including C₃ and C₄ native and improved pastures. The simulations presented here are not intended as an exhaustive analysis of the sites. Rather, they demonstrate the potential of the model to be integrated into detailed mitigation studies for all livestock grazing systems in Australia. I am confident the model will be of value in future applications and analysis of carbon, methane and nitrous oxide dynamics in Australian pastures.

5 References

- Cullen BR, Eckard RJ, Callow MN, Johnson IR, Chapman DF, Rawnsley RP, Garcia SC, White T, Snow VO. (2008). Simulating pasture growth rates in Australian and New Zealand grazing systems. *Australian Journal of Agricultural Research*, **59**, 761-768.
- Davidson EA, Verchot LV, Cattanio, JH, Ackerman, IL, Carvalho JEM (2000). Effects of soil water content on soil respiration in forests and cattle pastures of eastern Amazonia. *Biogeochemistry* **48**, 53-69.
- Grace PR, Jeffrey JN, Robertson GP, Gage SH (2006). SOCRATES—A simple model for predicting long-term changes in soil organic carbon in terrestrial ecosystems. *Soil Biology & Biochemistry* **38**, 1172–1176.
- Hurst DF, Griffith DWT, Cook GD (1994). Trace gas emissions from biomass burning in tropical Australian savannas. *Journal of Geophysical Research*, **99**, 441-456.
- Jeffrey SG, Carter JO, Moodie KB, Beswick AR (2001) Using spatial interpolation to construct a comprehensive archive of Australian climate data. *Environmental Modelling & Software* **16**, 309–330.
- Jenkinson, DS, (1990) The turnover of organic carbon and nitrogen in soil, *Philosophical Transactions, Royal Society of London B329*, 361-368.
- Johnson IR (2011). Testing and evaluating large-scale agricultural simulation models. MODSIM, 2011, Perth.
- Johnson IR, Parsons AJ, Ludlow MM (1989). Modelling photosynthesis in monocultures and mixtures. *Australian Journal of Plant Physiology*, **16**, 501-516.
- Johnson IR, Lodge GM, White RE (2003). The Sustainable Grazing Systems Pasture Model: description, philosophy and application to the SGS National Experiment. *Australian Journal of Experimental Agriculture*, **43**, pp 711-728.
- Johnson IR, Chapman DF, Snow VO, Eckard RJ, Parsons AJ, Lambert MG, Cullen BR (2008). DairyMod and EcoMod: biophysical pastoral simulation models for Australia and New Zealand. *Australian Journal of Experimental Agriculture*, **48**, 621-631.
- Johnson IR, France J, Thornley JHM, Bell MJ, Eckard RJ (2012). A generic model of growth, metabolism and body composition for cattle and sheep. In review.
- Johnson IR, Thornley JHM (1983). Vegetative crop growth model incorporating leaf area expansion and senescence, and applied to grass. *Plant, Cell and Environment*, **6**, 721-729.
- Johnson IR, Thornley JHM, Frantz JM, Bugbee B (2010). A model of canopy photosynthesis incorporating protein distribution through the canopy and its acclimation to light, temperature and CO₂. *Annals of Botany*, **106**, 735-749.
- IPCC (2006) '2006 IPCC Guidelines for National Greenhouse Gas Inventories, Volume 4, Agriculture, Forestry and Other Land Use.' (Intergovernmental Panel on Climate Change IGES, Japan)
- Li Z, Kelliher FM (2007). Methane oxidation in freely and poorly drained grassland soils and effects of cattle urine application. *Journal of Environmental Quality*, **36**, 1241-1248.
- Liedloff AC, Cook GD (2007). Modelling the effects of rainfall variability and fire on tree populations in an Australian tropical savanna with the Flames simulation model. *Ecological Modelling*, **201**, 269-282.
- Lodge GM, Johnson IR (2008). Agricultural drought analyses for temperate Australia using a biophysical pasture model. 1. Identifying and characterising drought periods. *Australian Journal of Agricultural Research*, **59**, 1049-1060.
- Oreskes N, Shrader-Frechette K, Belitz K. (1994). Verification, validation, and confirmation of numerical models in the earth sciences. *Science*, **263**, 641-646.
- McCaskill MR, Blair GJ (1988). Development of a simulation model of sulphur cycling in grazed pastures. *Biogeochemistry*, **5**, 165-181.
- Parton WJ, Steward JBW, Cole CV (1988). Dynamics of C, N, P and S in grassland soils: a model. *Biogeochemistry* **5**, 109-131.

- Parton WJ, Stewart JWB, Cole CV (1998). Dynamics of C, N, P and S in grassland soils: a model. *Biogeochemistry* **5**, 109-131.
- Probert ME, Dimes JP, Keating BA, Dalal RC, Strong WM (1998). APSIM's water and nitrogen modules and simulation of the dynamics of water and nitrogen in fallow systems. *Agricultural Systems* **56(1)**, 1-28.
- Russell-Smith J, Murphy BP, Meyer CP, Cook GD, Maier S, Edwards AC, Schatz J, Brocklehurst P (2009). Improving estimates of savanna burning emissions for greenhouse accounting in northern Australia: limitations, challenges, applications. *International Journal of Wildland Fire*, **18**, 1-18.
- Skjemstad, JO, Spouncer, LR, Cowie, B, Swift, RS (2004) Calibration of the Rothamsted organic carbon turnover model (RothC ver. 26.3), using measurable soil organic carbon pools. *Australian Journal of Soil Research* **42**, 79-88.
- The Land* (16 July, 2010). *Error in Snowy soils carbon report*.
- Thornley, J.H.M. 1998. *Grassland Dynamics: An Ecosystem Simulation Model*. CAB International. Wallingford, UK.
- Van Veen JA, Paul EA (1981). Organic carbon dynamics in grassland soils. 1. Background information and computer simulation. *Canadian Journal of Soil Science* **61**, 185-20.
- Van Veen JA, Ladd JN, Frissel MJ (1984). Modelling C and N turnover through the microbial biomass in soil. *Plant and Soil* **76**, 257-74.
- Van Veen JA, Ladd JN, Amato M (1985). Turnover of carbon and nitrogen through the microbial biomass in a sandy loam and a clay soil incubated with C-14 glucose and N-15 ammonium sulfate under different moisture regimes. *Soil Biology and Biochemistry* **17**, 747-56.
- Whitehead DC (1995) 'Grassland nitrogen.' (CAB International: Wallingford, UK)

6 Acknowledgements

I am grateful to Richard Eckard, Tony Parsons, Annette Cowie, Mathew Bell, Garry Cook, Adam Liedloff, Ram Dalal, Diane Allen, Joe Scanlan, Ed Charmley and Luciano Gonzalez for helpful discussions. All errors and omissions are mine.

7 Appendix

7.1 Appendix 1: Model Structure

A brief description of the structure of the SGS Pasture Model is presented. It is a daily time-step model that includes pasture growth and utilization by grazing animals, animal metabolism and growth, water and nutrient dynamics, and options for pasture management, irrigation and fertilizer application. Note that the model has the same underlying biophysical structure as DairyMod (Johnson *et al.*, 2008), which has been developed to address questions relevant to the dairy industry.

- The pasture growth module includes calculations of light interception and photosynthesis; growth and maintenance respiration, nutrient uptake and nitrogen fixation, partitioning of new growth into the various plant parts, development, tissue turnover and senescence, and the influence of atmospheric CO₂ on growth. The model allows up to five pasture species in any simulation, which can be annual or perennial, C₃ or C₄, as well as legumes.
- The water module accounts for rainfall and irrigation inputs that can be intercepted by the canopy, surface litter or soil. The required hydraulic soil parameters are saturated hydraulic conductivity, bulk density, saturated water content, field capacity or drained upper limit, wilting point and air-dry water content.

- Different soil physical properties can be defined through the soil profile. The nitrogen module incorporates the dynamics of NO_3 and NH_4 , including leaching, and soil organic matter. Gaseous losses of nitrogen through volatilization and denitrification are included.
- The animal module has a sound treatment of animal intake and metabolism including growth, maintenance, pregnancy and lactation. There are options to select sheep (wethers or ewes with lambs), cattle (steers or beef cows with calves), and dairy cows. Methane emissions are included.
- The farm management module describes the movement of stock around the paddocks as well as strategies for conserving forage, and incorporates a wide range of rotational grazing management strategies that are used in practice. There are options for single- and multi-paddock simulations that can each be defined independently to represent spatial variation in soil types, nutrient status, pasture species, fertilizer and irrigation management.
- The model has a complete description of the system carbon dynamics as well as non- CO_2 (methane and nitrous oxide) emissions.

The model uses rainfall, maximum and minimum temperature, solar radiation, vapour pressure, as well as site latitude and elevation. All simulations presented here use a fixed 2 m s^{-1} wind speed and 380 ppm atmospheric CO_2 concentration.

A key characteristic of the model is the interaction between the individual modules as illustrated in Fig. 1 in the main text.

As with most biophysical simulation models, this model is subject to continual review and refinement in light of on-going model application. A brief description of the modules is therefore presented, with details presented for recent developments. Note that SI units are used throughout the analysis although results will be presented on a per ha basis.

A fundamental objective in the development of the SGS Pasture Model has been to ensure that model parameters have an underlying biophysical interpretation and that the parameter values defining biophysical processes are generic and not specific to individual sites. For example, with a pasture species such as phalaris, the same set of physiological parameters can be applied at any location and, though different varieties may have different physiological characteristics, key parameters can be modified with knowledge of the characteristics of each variety. This approach has been applied, for example, by Cullen *et al.* (2008) who, with the knowledge that later varieties had better growth at low temperatures, were able to model both old and more recent varieties of perennial ryegrass. Furthermore, all model parameters are directly accessible from the model interface so that it is quite straightforward for model users to adjust parameter values and explore the corresponding responses.

7.1.1 Pasture growth

The pasture growth model is driven by photosynthesis, with canopy photosynthesis and respiration described according to Johnson *et al.* (2010). According to this model, leaf gross photosynthesis in response to photosynthetic photon flux (PPF) is described using the non-rectangular hyperbola, with the parameters of this equation being related to temperature and plant nitrogen status. Growth and maintenance respiration components are included. Different respiratory costs for synthesising cell wall material and protein, and maintenance respiration depends on plant protein concentration. The tissue turnover dynamics are based on the model structure of Johnson and Thornley (1983) which has been widely used, and developed, both for the present model and other models, such as the Hurley Pasture Model (Thornley, 1998).

For multiple species, light interception is described according to Johnson *et al.* (1989), but now allowing for pasture species to have prescribed height as a function of whole canopy leaf area index. Carbon partitioning to the roots is influenced by soil water status and nitrogen concentration.

7.1.2 Soil Hydrology and evapotranspiration

Soil water infiltration is defined using a capacitance multi-layer approach. The top 4 layers are each 5 cm and subsequent layers 10 cm. The flux of water, q m water d⁻¹ is given by

$$q = K_{sat} \left(\frac{\theta}{\theta_{sat}} \right)^\sigma \quad (1)$$

where θ m³(water) m⁻³(soil) the volumetric soil water content, θ_{sat} the saturated water content, K_{sat} m d⁻¹ is the saturated hydraulic conductivity, which is the value of q when $\theta = \theta_{sat}$, and σ is a flux coefficient. θ_{sat} is calculated from the soil bulk density, ρ_b kg m⁻³(soil) according to the standard equation

$$\theta_{sat} = 1 - \frac{\rho_b}{\rho_p} \quad (2)$$

where ρ_p is the particle density taken to be 2,650 kg m⁻³. In order to calculate σ , a drainage point θ_{dp} is defined with corresponding prescribed flux q_{dp} so that σ is given by

$$\sigma = \frac{\ln(q_{dp}/K_{sat})}{\ln(\theta_{dp}/\theta_{sat})} \quad (3)$$

In the model, the value

$$q_{dp} = 10^{-4} \text{ m d}^{-1} \quad (4)$$

which is equivalent to 0.1 mm d⁻¹ is used so that, for example, if $K_{sat} = 0.1$ m d⁻¹, $\rho_b = 1,400$ kg m⁻³, $\theta_{dp} = 0.4$, then $\theta_{sat} = 0.47$ and $\sigma = 41.9$. Equation (1) is illustrated in Fig. A1, on linear and log scales, with these parameters.

Soil water infiltration is calculated using eqn (1) at each layer in the soil. This involves selecting a sub-daily time-step to ensure the solution is stable and smooth. Details and examples are presented in Johnson (2012). This approach is simple to work with and provides a realistic distribution of water through the profile for different locations and soil types (eg Lodge and Johnson, 2008).

Soil water infiltration is defined using a capacitance multi-layer approach. The top 4 layers are each 5 cm and subsequent layers 10 cm. The flux of water, q m water d⁻¹ is given by

$$q = K_{sat} \left(\frac{\theta}{\theta_{sat}} \right)^\sigma \quad (5)$$

where θ m³(water) m⁻³(soil) the volumetric soil water content, θ_{sat} the saturated water content, K_{sat} m d⁻¹ is the saturated hydraulic conductivity, which is the value of q when $\theta = \theta_{sat}$, and σ is a flux coefficient. θ_{sat} is calculated from the soil bulk density, ρ_b kg m⁻³(soil) according to the standard equation

$$\theta_{sat} = 1 - \frac{\rho_b}{\rho_p} \quad (6)$$

where ρ_p is the particle density taken to be $2,650 \text{ kg m}^{-3}$. In order to calculate σ , a drainage point θ_{dp} is defined with corresponding prescribed flux q_{dp} so that σ is given by

$$\sigma = \frac{\ln(q_{dp}/K_{sat})}{\ln(\theta_{dp}/\theta_{sat})} \quad (7)$$

In the model, the value

$$q_{dp} = 10^{-4} \text{ m d}^{-1} \quad (8)$$

which is equivalent to 0.1 mm d^{-1} is used so that, for example, if $K_{sat} = 0.1 \text{ m d}^{-1}$, $\rho_b = 1,400 \text{ kg m}^{-3}$, $\theta_{dp} = 0.4$, then $\theta_{sat} = 0.47$ and $\sigma = 41.9$. Equation (1) is illustrated in Fig. A1, on linear and log scales, with these parameters.

Soil water infiltration is calculated using eqn (1) at each layer in the soil. This involves selecting a sub-daily time-step to ensure the solution is stable and smooth. Details and examples are presented in Johnson (2012). This approach is simple to work with and provides a realistic distribution of water through the profile for different locations and soil types (eg Lodge and Johnson, 2008).

7.1.3 Soil organic matter and nutrient dynamics

Soil organic matter dynamics are generally modelled by using pools of organic matter with different turnover rates. Early models of this type were developed by Van Veen & Paul (1981) and Van Veen *et al.* (1984, 1985), McCaskill and Blair (1988), Parton *et al.* (1988). Since then, the multi-pool approach has been extensively applied with well-known models being APSIM (Probert *et al.* 1998), RothC (Jenkinson 1990), CENTURY (Parton *et al.* 1998), and SOCRATES (Grace *et al.*, 2006). A fundamental challenge with soil carbon models comprising several pools is that it is possible to get similar overall carbon dynamics with different rates of input and turnover, and so we must continually assess all aspects of the soil carbon dynamics in the model including the description of plant growth and senescence as it feeds into the soil carbon.

The approach in the model has been to simplify the description of soil organic matter dynamics to include dynamic fast and slow turn-over pools, plus an inert component. The fast and slow pools are sometimes referred to as *particulate organic matter* and *humus soil carbon*. The inert carbon pool, which is essentially charcoal, is not subject to turnover. Keeping the model relatively simple avoids having to define a large number of parameters that are likely to have strong interactions and are difficult to estimate. The only parameters required are the decay rate constants for the fast and slow pools (proportion that decays per unit time), their efficiency of decay (proportion of carbon respired during decay), and the transfer rate from the fast to slow pool. The N concentration of the inputs are also required, and are calculated dynamically in the model. Soil carbon dynamics are also affected by temperature and soil water status. Soil carbon dynamics are driven by inputs from the plant material, and its digestibility.

The model is illustrated in Fig. A2. There are two dynamic pools representing fast and slow turnover carbon, $W_{F,soil}$ and $W_{S,soil}$ kg C m^{-3} , and a third inert pool which is primarily charcoal. Note that SI units are used throughout the model, although results are converted to familiar units (such as t C ha^{-1} in the top 30cm soil). Inputs from dead plant material and dung are transferred to $W_{F,soil}$. This is subject to decay and also transfer to $W_{S,soil}$, which also decays but at a slower rate. During decay, carbon is respired as CO_2 , with the remainder going to the fast turnover pool. Note that restricting our analysis to these three pools is consistent with current recommended measureable soil carbon pools (Skjemstad *et al.* 2004).

Although the model only considers two dynamic pools, the decay characteristics of $W_{F,soil}$ are related to the digestibility of the inputs so that litter and dead roots from less digestible pastures will decay at a slower rate than more digestible inputs.

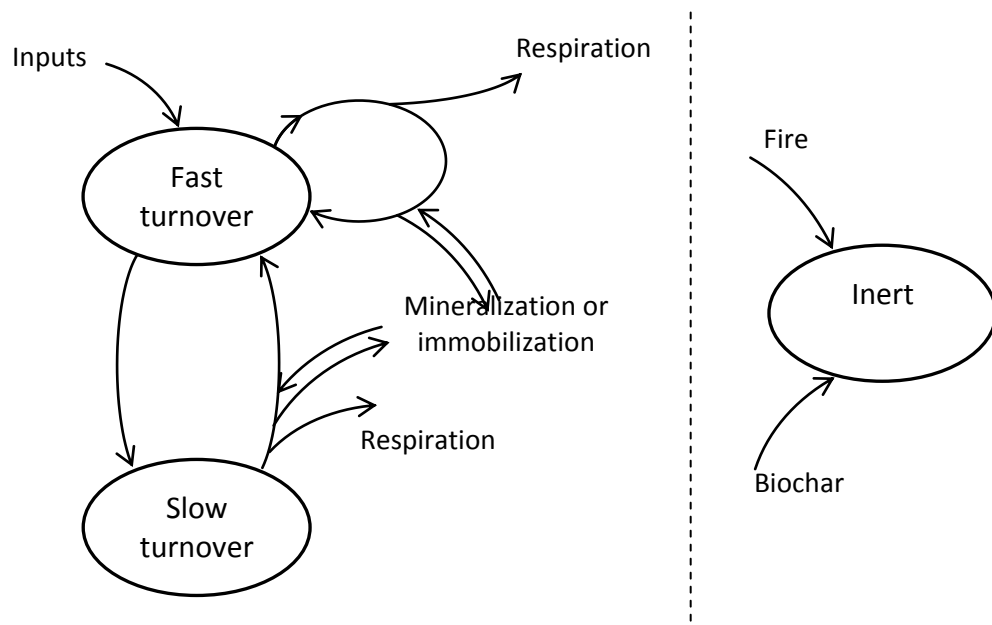


Figure A2. Overview of the soil carbon dynamics.

The general approach is to define organic matter decay of pool W_C kg C m⁻³ as kW_C where k , d⁻¹, is a decay coefficient. Decay occurs with efficiency Y so that YkW_C kg C m⁻³ is retained and $(1 - Y)kW_C$ respired. It is assumed that the retained carbon for both fast and slow pool decay is transferred to the fast pool.

Denoting the carbon mass in the fast and slow turn-over pools by $W_{F,C}$ and $W_{S,C}$ kg C m⁻³ respectively, their dynamics are described by

$$\frac{dW_{F,C}}{dt} = I_C - k_{FS}W_{F,C} - k_F(1 - Y_F)W_{F,C} + Y_S k_S W_{S,C} \quad (9)$$

$$\frac{dW_{S,C}}{dt} = k_{FS}W_{F,C} - k_S W_{S,C} \quad (10)$$

where k_F and k_S (d⁻¹) are the decay rates for the fast and slow pools, k_{FS} (d⁻¹) is the transfer coefficient for movement from the fast to slow pool, Y_F and Y_S are the dimensionless efficiencies of fast and slow organic matter decay, and I_C (kg C m⁻³ d⁻¹) is the rate of carbon input, and t (d) is time. The corresponding respiration is

$$R = (1 - Y_F)k_F W_{F,C} + (1 - Y_S)k_S W_{S,C} \quad (11)$$

Now consider the associated nitrogen dynamics. (Other nutrients can be treated similarly.) The decay of organic matter is assumed to be through digestion by biomass. The biomass pool is not modelled explicitly, and is taken to be part of the fast pool. Defining the N fraction of the biomass as $f_{B,N}$, kg N (kg C)⁻¹ which is taken to be a fixed quantity, and the corresponding N fractions for the pools as $f_{F,N}$ and $f_{S,N}$, which will be variables that depend on the inputs and decay parameters, the nitrogen dynamics corresponding to eqns (9) and (10) are

$$\frac{dW_{F,N}}{dt} = I_N - k_{FS}W_{F,N} - k_F W_{F,N} \left(1 - Y_F \frac{f_{B,N}}{f_{F,N}} \right) + Y_S k_S \frac{f_{B,N}}{f_{S,N}} \quad (12)$$

$$\frac{dW_{S,N}}{dt} = k_{FS}W_{F,N} - k_S W_{S,N} \quad (13)$$

The associated N mineralization rate, which is the flux of N from the soil organic matter into the ammonium pool, is

$$M_N = k_F W_{F,N} \left(1 - Y_F \frac{f_{B,N}}{f_{F,N}} \right) + k_S W_{S,N} \left(1 - Y_S \frac{f_{B,N}}{f_{S,N}} \right) \quad (14)$$

If this is negative then immobilization of inorganic nitrogen occurs and it is assumed that this nitrogen can be supplied either from the NH₄ or NO₃ pools.

These relatively simple equations completely define the soil organic matter dynamics, including carbon assimilation and respiration as well as nitrogen mineralization or immobilization. We have used nitrogen fractions of organic matter and biomass rather than C:N ratios which are more common. The analysis is clearer to work with using fractions, although the C:N ratio is the inverse of the N fraction. Thus, the default value for $f_{B,N}$ is taken to be 1/8 which is equivalent to a C:N ratio in biomass of 8. In the simulations that follow, results will be shown as C:N ratios. Organic matter dynamics are influenced by soil water status and temperature (Davidson *et al.*, 2000). The rate constants k_{FS} , k_F , k_S are defined by

$$k = \phi_H \phi_T k_{ref} \quad (15)$$

where ϕ_H and ϕ_T are dimensionless water and temperature functions respectively, and k_{ref} is a reference value for each of the rate constants defined at non-limiting soil water conditions and 20°C. Estimating these responses from experimental data is difficult owing to variation in the data. It is assumed that soil biological processes are unrestricted by available water at water potentials greater than -100kPa which, using the Campbell water retention function to relate water potential to content, can be shown to occur at the average of the drainage point and wilting point in the soil (Johnson *et al.*, 2012). Denoting this by θ_{100} , the generic function for ϕ_H is illustrated in Fig. 4. A similar equation is used for ϕ_T , which is also illustrated in Fig. A3. The mathematical details of these equations are described by Johnson (2012). In the model, users can adjust both these curves. For ϕ_H the wilting point and drainage point are prescribed for different regions in the soil profile, and for ϕ_T the minimum and optimum temperatures can also be adjusted.

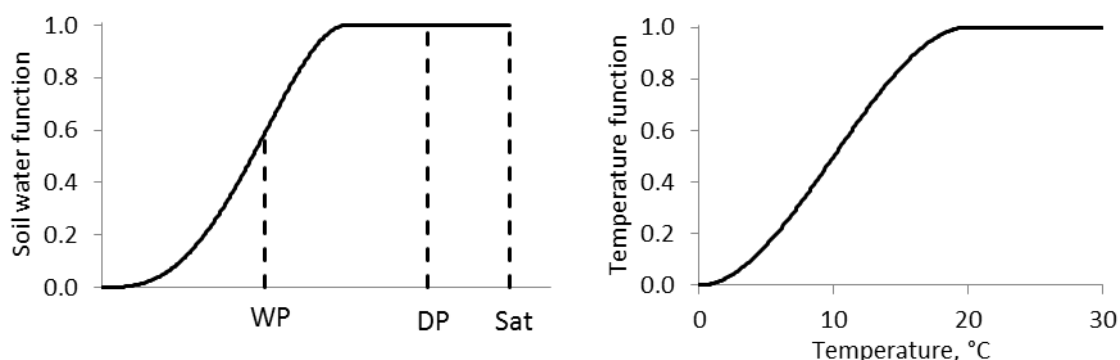


Figure A3. Soil water (left) and temperature (right) response functions, ϕ_H and ϕ_T respectively.

Now consider the influence of the quality of organic matter inputs through plant and root senescence on organic matter dynamics. For each plant species, the digestibility of both the live and dead plant tissue is prescribed. The value for the dead material is taken to influence both the decay coefficient, k_F , and efficiency of breakdown, Y_F , of the fast pool. This is done on a pro-rata basis, so that the decay coefficient on day t is related to the value on day $t-1$ by

$$k_{F,t} = \left[k_{F,ref} \Delta W_{C,in} \frac{\delta_{in}}{\delta_{ref}} + k_{F,t-1} W_{F,C} \right] / (W_{F,C} + \Delta W_{C,in}) \quad (16)$$

where $W_{F,C}$ is the initial mass of carbon in the fast pool, $\Delta W_{C,in}$ is the carbon input with digestibility δ_{in} , δ_{ref} is a reference digestibility (taken to be 0.4), and k_{ref} is the reference decay rate for material with digestibility δ_{ref} . The efficiency is then calculated according to

$$Y_F = Y_{F,ref} \frac{k_F}{k_{F,ref}} \quad (17)$$

According to this scheme, the fast pool decay characteristics vary in relation to the quality of senescent plant material input, which avoids having multiple pools with relatively rapid turnover rates.

It is assumed that the decay rates for the fast and slow pools are independent of soil type, whereas the transfer from the fast to slow pool is taken to be related to the soil clay fraction. Thus,

$$k_{FS} = k_{FS,ref} \frac{\gamma}{\gamma_{ref}} \quad (18)$$

where γ is the clay fraction and γ_{ref} is a reference value so that $k_{FS} = k_{FS,ref}$ when $\gamma = \gamma_{ref}$. By default, $\gamma_{ref} = 0.5$.

This completely defines the soil organic matter dynamics including carbon accumulation and respiration, N mineralization and immobilization, and the influence of soil water, temperature, and quality of inputs. In general, the decay rate will decline as the soil dries below -100 kPa and 20°C. Both the rate and efficiency of decay of the fast turnover pool will decline with decreasing quality of organic matter inputs, as defined by digestibility.

Half-life and mean residence time

The decay rates of soil organic matter pools are characterised by the decay rate k parameters in the above equations, which have dimensions of time^{-1} . However, these parameters do not lend themselves to intuitive biophysical interpretation.

For linear decay systems of the form used here, where the time course of pool W with decay coefficient k , with no inputs to the system, is

$$\frac{dW}{dt} = -kW \quad (19)$$

which has solution

$$W = W_0 e^{-kt} \quad (20)$$

where W_0 is the initial value of W . This is, of course, simple exponential decay. The *half-life* is the time for W to reach half its initial value, and is simply given by

$$h = \frac{\ln(2)}{k} = \frac{0.69}{k} \quad (21)$$

The term *mean residence time* is also used. This again is derived from exponential decay in refers to the mean time that an element, or constituent, of the pool remains in the pool, and is given by

$$r = \frac{1}{k} \quad (22)$$

so that

$$r = \frac{h}{0.69} \quad (23)$$

Thus the terms are linearly related.

My preference is for half-life and this is used in the present analysis.

7.1.4 Soil methane oxidation

It is well established that atmospheric CH_4 can be oxidized by microbes in the soil. There has been discussion in the press (*The Land*, 2010) regarding this process with suggestions it could be significant. This article reported work from Sydney University, though I have been unable to find any presentation of these results in the scientific literature. The article actually points out that the initial calculations were in error by a factor of 1000 due to a mix up between milli and micro units. Nevertheless, it was suggested that CH_4 oxidation rates of the order of $7.6 \text{ kg CH}_4 \text{ ha}^{-1} \text{ yr}^{-1}$ occur in high country Snowy Mountains soils. These values are significantly greater than those reported in the literature. For example, Li and Kelliher (2007) measured CH_4 oxidation rates in freely and poorly drained soils on an intensively managed dairy farm in New Zealand. The highest rates were $1.8 \text{ kg CH}_4 \text{ ha}^{-1} \text{ yr}^{-1}$ which occurred in the poorly drained soils. While CH_4 oxidations rates are known to be higher in pristine forests, these rates for pastures are consistent with other values reported in the literature (see Li and Kelliher, 2007).

Oxidation of CH_4 may have a role to play on continent scale GHG calculations, but there is little evidence to suggest that it is significant for grazed pasture systems. In addition, the actual rates are trivial in comparison with carbon fixation through photosynthesis and so have no significant role in the overall carbon dynamics of a grazed pasture. For example, in the simulations presented below, the average annual carbon fixed through net photosynthesis at Hamilton was $6.9 \text{ t C ha}^{-1} \text{ yr}^{-1}$, and a CH_4 oxidation rate of $1.8 \text{ kg CH}_4 \text{ ha}^{-1} \text{ yr}^{-1}$ corresponds to less than 0.02% of the carbon fixed through photosynthesis.

In summary, CH₄ oxidation rates are negligible in terms of the overall carbon fixed through photosynthesis and the overall carbon balance of the system, and, as they are not anthropogenic, do not form part of the current accounting system. It is therefore my recommendation that we do not incorporate CH₄ oxidation in the model.

7.1.5 Fire

Fire is an important factor for extensive grazing systems in the Northern Territory. As dead plant material burns, the carbon is emitted primarily as CO₂ and CO, with trace amounts of CH₄. Nitrogen is emitted mainly as N₂, NO_x (oxides of nitrogen), and NH₃, with small amounts of N₂O. There is also production of ash. The CH₄ and N₂O emissions are very small components in the overall C and N dynamics, but they are important greenhouse gases. The model has therefore been developed to account for these emissions. CH₄ and N₂O emissions from burning pastures are included in the model since they represent a source of anthropogenic emission for non-accidental burning of pastures.

The treatment of the effects of fire here is relatively simple, focussing primarily on the burning of pasture. The impact of fire on tree dynamics is complex and has been thoroughly modelled by Adam Leidloff and Garry Cook of CSIRO, Darwin (Liedloff and Cook, 2007). Their model, 'Flames', describes the impact of fire on the eucalypt dominated tree component of northern Australia savannas and provides a framework to address issues such as fire frequency and intensity on tree growth and population dynamics. As discussed later, there is potential to work with both models together. The following description of the implementation of the impacts of fire on GHG dynamics in pastures is taken from these references, as well as Hurst *et al.* (1994) and Russell-Smith *et al.* (2009).

The scheme for the impact of burning on C and N dynamics is illustrated in Fig. 3, with parameters listed in Table 1 along with default values. The key parameters affecting GHG emissions are the emission factors for CH₄ and N₂O, and these are taken from latest DCCEE CFI *Methodology for savanna burning* (Cook, *pers comm*), which are revised values from earlier methodologies. Note that the burning efficiency, which is the proportion of dry weight that is burnt, will vary across a landscape, with some areas being unaffected by fire. For the present analysis, the focus is on areas that have been burnt and so the burning efficiency is taken to be close to 1. However, this parameter can be readily adjusted on the model interface. Accounting for all of the N during burning is difficult, partly due to the fact that N₂ from fire cannot be directly measured. In the model, once N₂O has been calculated, it is assumed that the burnt ash has a fixed N:C ratio, which is then used to estimate other gaseous N losses. Ash that is retained on the paddock is transferred directly to the inert soil carbon pool in the top soil layer.

Table A1. Parameters used in the treatment of the impact of fire on burning pastures. The emission factors for CH₄ and N₂O are from the latest DCCEE CFI *Methodology for savanna burning* (Cook, *pers comm*).

Parameter	Definition	Default value
ϵ_{fire}	Burning efficiency, proportion of dry weight that is burnt	0.95
β_{CH_4}	Emission factor for CH ₄	0.0015 kg C as CH ₄ (kg C in d.wt) ⁻¹
β_{CO_x}	Emission factor for non CH ₄ gases, primarily CO ₂ and CO	0.96 kg C (kg C in d.wt) ⁻¹
β_{N_2O}	Emission factor for N ₂ O	0.0075 kg N as N ₂ O (kg N in d.wt) ⁻¹
$f_{N,ash}$	N:C ratio in burnt ash	1/30 kg N (kg C) ⁻¹
γ_{ash}	Proportion of ash retained on the paddock during burning	0.5

The model makes no attempt to predict the actual occurrence of fire, which can result from intentional or accidental burning, as well as lightning. Fire frequency is specified in the model, as well as the day and month of burning. Fires can either be regular or random. If the user selects random fires, then the model uses a random number generator to select years when fire can occur. For example, with random fires every 5 years, the model generates a random integer between 1 and 5 on the day of potential burning and if this number is 5 then the fire occurs.

Illustrations of the impact of burning are presented later. However, it is worth considering the general implication of the choice of model parameters on CH₄ emissions. If 1 t d.wt is burnt and it is 45% C, then the CH₄ emission is 0.85 kg CH₄. For a steer eating an average of 7 kg d.wt d⁻¹, the corresponding CH₄ emission is 51 kg CH₄ year⁻¹. Thus, the emissions from one steer are roughly equivalent to the burning of 60 t d.wt. While emissions from fire are significant, particularly when large areas are burnt, these figures give an indication of the relative magnitude of methane from fire and stock.

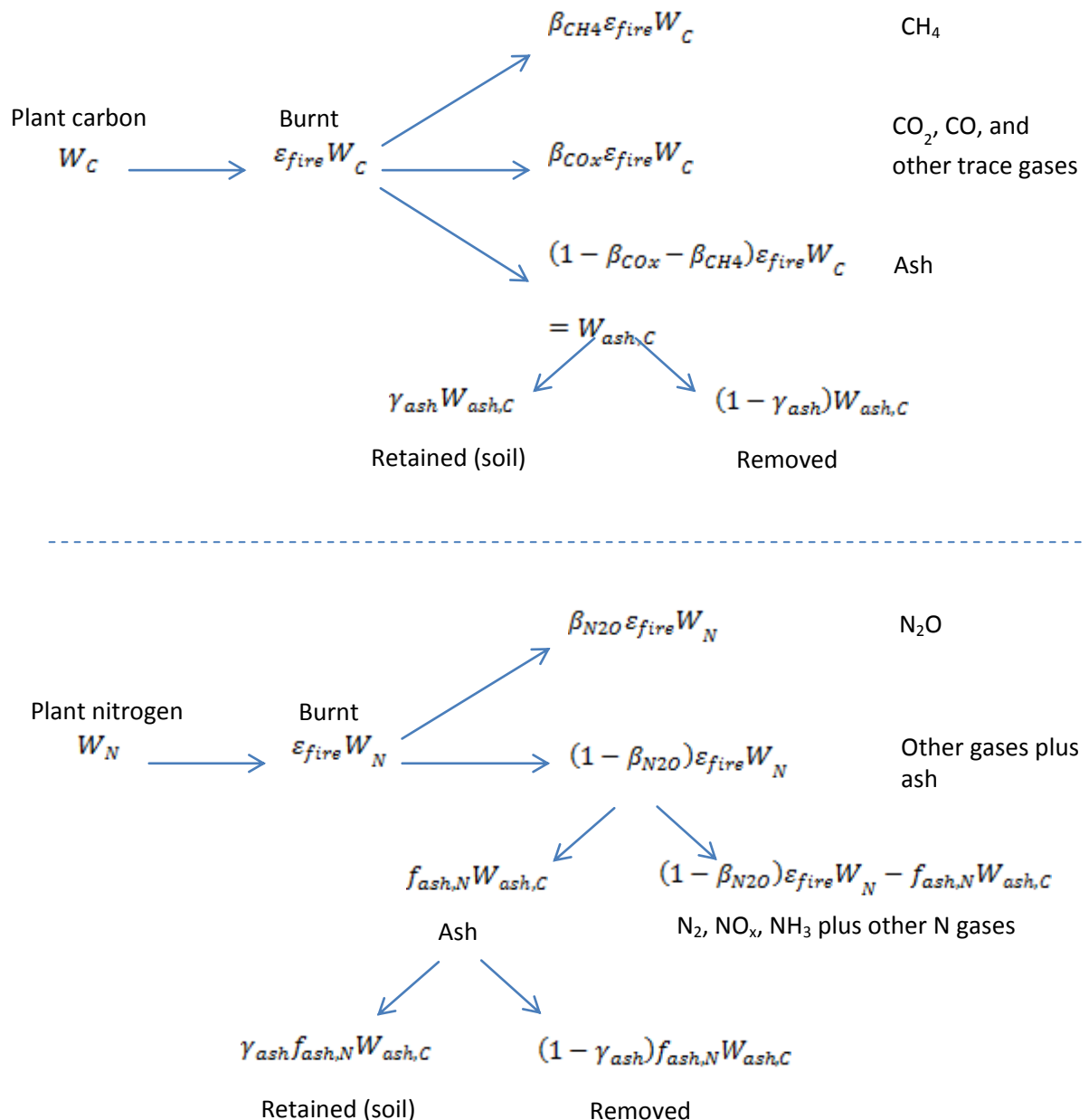


Figure A4. Schematic representation of carbon and nitrogen dynamics during pasture burning.

W_C and W_N are the plant carbon and nitrogen, and $W_{ash,C}$ is the carbon produced as ash.

See text for details and Table 1 for parameter definitions and default values.

7.1.6 Impact of trees on pasture growth

In discussions throughout the project and at the modelling workshop in Brisbane (May, 2012), it was decided that it is not appropriate to incorporate a full tree growth model in the SGS Pasture Model.

There are several well developed models for assessing the potential of trees for carbon sequestration. In addition, the impact of fire on tree stands has been modelled in detail by Liedloff and Cook, as discussed above.

Trees do, however, play a role in pasture production, primarily through their use of water and also by shading the plants. These effects have been incorporated in the model by assuming a constant tree ground cover. Light interception and transpiration of the trees is then incorporated in the model using the same methodology as for pastures. It is assumed that the trees are in carbon equilibrium, so that inputs to the soil carbon from tree litter and material are matched by soil organic matter decay of tree material. While this is a simple treatment, it does allow for the impact of trees on pasture growth while avoiding excessive complexity in incorporating a full tree physiological model. It should be noted that possible benefits of trees through providing shelter for stock are not addressed in the model.

To implement the effect of trees on pasture productivity, the user therefore simply prescribes the tree ground cover.

7.1.7 Animal intake, metabolism, growth and nutrient returns

The animal model is described in Johnson *et al.* (2012). The model includes protein, water and fat components of body composition, and energy is utilized for growth of new tissue, resynthesis of degraded protein, and the energy required for physical activity. Pregnancy and lactation are also incorporated where relevant. For the present analysis, all simulations are for set-stocking and so, to keep the management options as simple as possible, we do not include animal growth, but assume the animal is always at a fixed mature weight, so that energy requirement is then calculated in relation to mature body weight. Dry matter intake requirement is then determined by energy requirement and pasture digestibility. Actual intake then depends on available pasture and potential intake which, in turn, declines with digestibility.

Since, for the present simulations, the animal weight is taken to be fixed, all carbon intake, after CH₄ and CO₂ emissions through fermentation and respiration respectively are taken into account, is assumed to be excreted as dung. It is further assumed that there is no net change in animal N content so that all N intake is excreted. Dung is taken to have a fixed N concentration with all excess N excreted in urine (Whitehead 1995). If C and N outputs do not meet this fixed concentration, then the N concentration in dung is reduced and there is no N in the urine.

Methane emissions are assumed to be a fixed proportion of animal intake on an energy basis which, for pastures, is taken to be 6% of the gross energy intake emitted as methane. Taking the IPCC value of 18.45 MJ kg⁻¹ for gross energy content of plant dry weight, and 55.65 MJ kg⁻¹ for methane (IPCC 2006), this corresponds to 19.9 g CH₄ (kg d.wt forage intake)⁻¹.

7.2 Appendix 2 GHG dynamics in pasture systems

The complete carbon balance in the system, ΔC , can be defined as:

$$\Delta C = P_{net} - R_{litter} - R_{dung} - R_{soil} - R_{animal} \quad (24)$$

where P_{net} is the rate of net photosynthesis and the R terms are respiration or fermentation with associated subscripts. All terms have units of mass of C per unit area per unit time. Note that R_{animal} includes both carbon emission as CO₂ through animal respiration and CH₄ through fermentation, both expressed in carbon units.

In practice, annual dynamics in $\text{t C ha}^{-1} \text{ yr}^{-1}$ are used: in the SGS model all calculations are made on a daily basis which are then aggregated to give monthly or annual totals. For GHG analyses, CO_2e dynamics, $\Delta\text{CO}_2\text{e}$ (with units CO_2e per time), are calculated, as defined by:

$$\Delta\text{CO}_2\text{e} = \frac{44}{12} \Delta C_{\text{soil}} - \gamma_{\text{CH}_4} R_{\text{animal,CH}_4} - \gamma_{\text{N}_2\text{O}} D_{\text{N}_2\text{O}} \quad (25)$$

where the ΔC_{soil} is the change in soil organic carbon, $R_{\text{animal,CH}_4}$ is the animal CH_4 emission, $D_{\text{N}_2\text{O}}$ is the rate of denitrification as N_2O , the fraction $44/12$ converts carbon to CO_2 and the γ coefficients are the CO_2e conversion coefficients for methane and nitrous oxide. These are taken to be 21 and 310 respectively, as in the IPCC Second Assessment Report. These coefficients are under continual review and it is straightforward to change them in the model. Note that eqn (25) does not include plant, litter or dung carbon dynamics directly, although these will affect the soil carbon dynamics. It is therefore not a true mass balance, but captures the net impact of the pasture system on the GHG emissions.

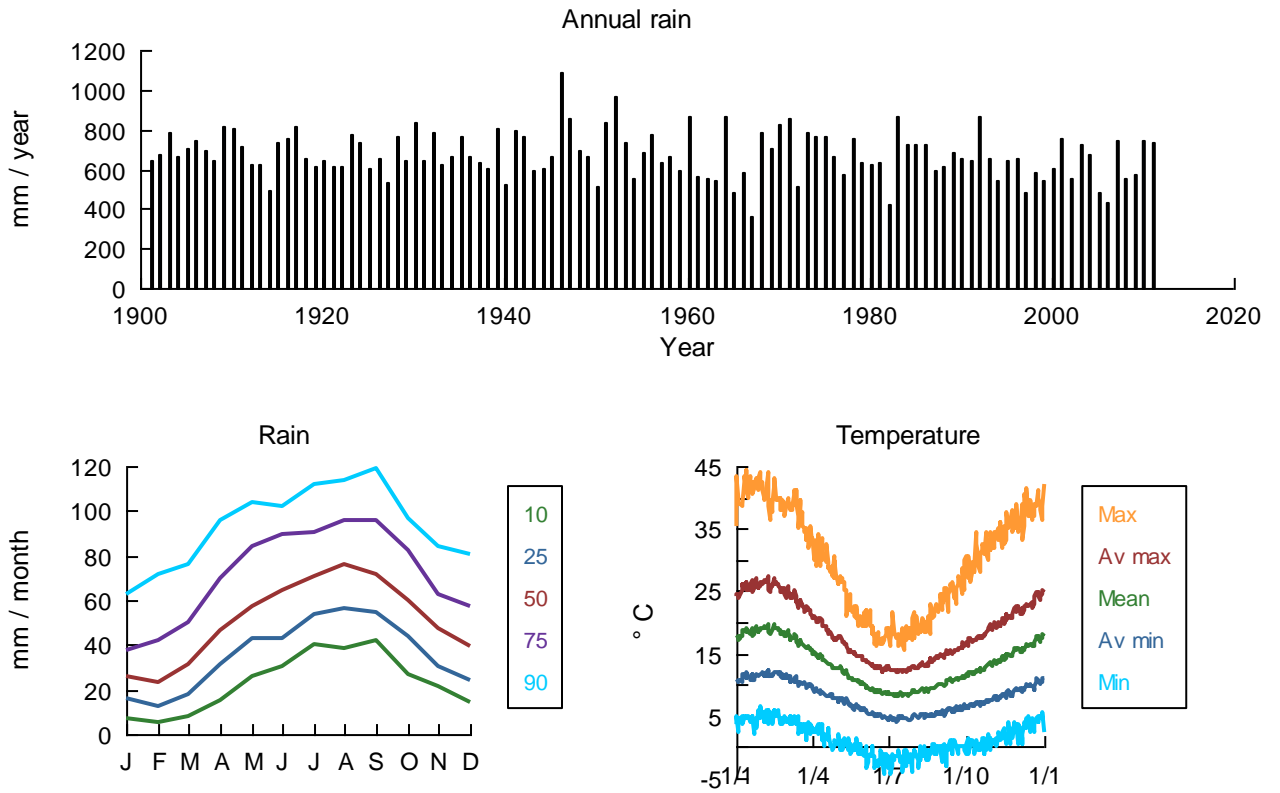
This description of GHG dynamics for the paddock, through the calculation of $\Delta\text{CO}_2\text{e}$, does not include estimates of off-site impacts through denitrification that may occur from N losses through leaching or volatilization (indirect N_2O emissions; IPCC 2006), although both leaching and volatilization are calculated in the model. The aim here is to focus on the paddock dynamics, but the model includes these other losses that can be used to estimate off-site impacts.

7.3 Site characteristics

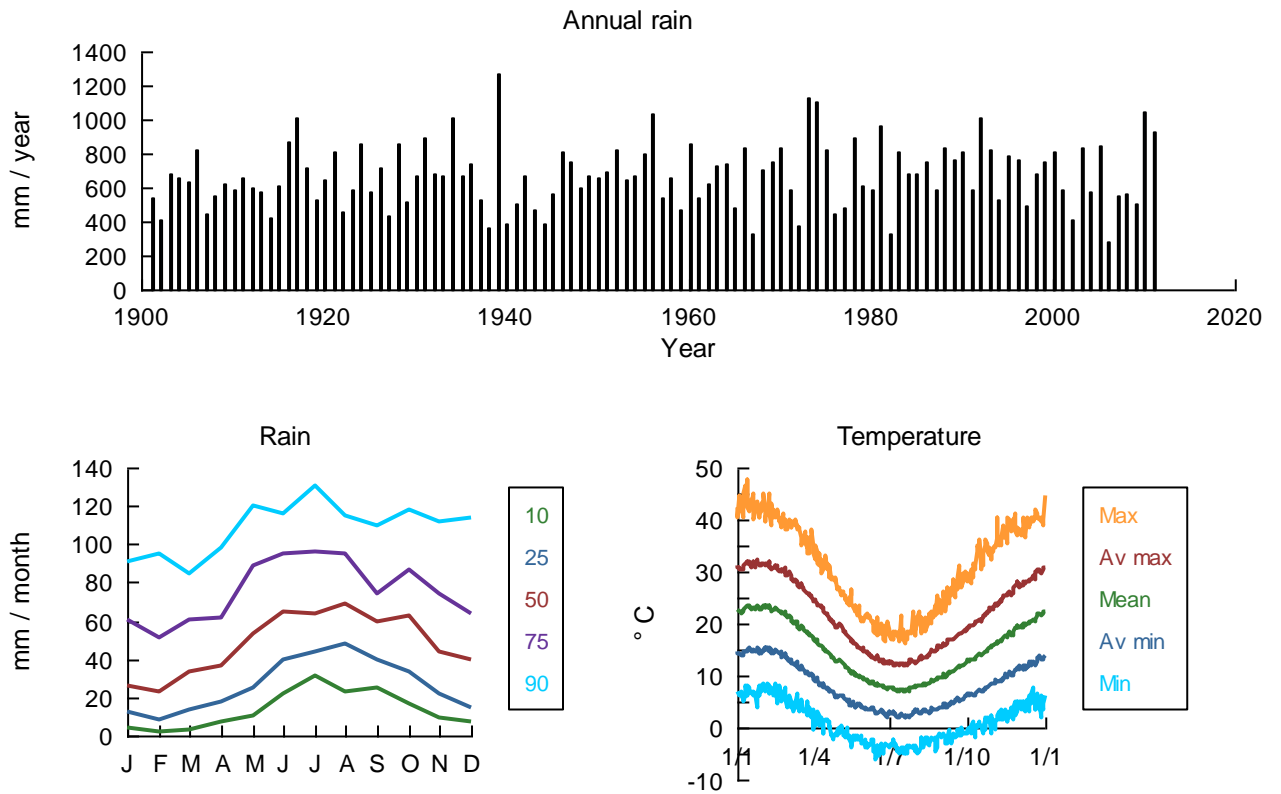
The following graphs show a summary of the climate characteristics for each site listed in Table 2 for the period 1901 to 2011 inclusive from the SILO database (Jeffrey *et al.*, 2001). The illustrations are for the annual rainfall, monthly rainfall percentiles and daily temperature variation. The rainfall graphs show continuous lines through percentiles, but it must be noted for example that a sequence of 90 percentile months is entirely different to a 90 percentile year. The temperature graphs include, for each day of the year:

- The maximum recorded temperature;
- The average of the maximum daily temperature;
- The average of the daily average temperature which, in turn is the average of the daily maximum and minimum temperature;
- The average of the minimum daily temperature;
- The minimum of the minimum temperature.

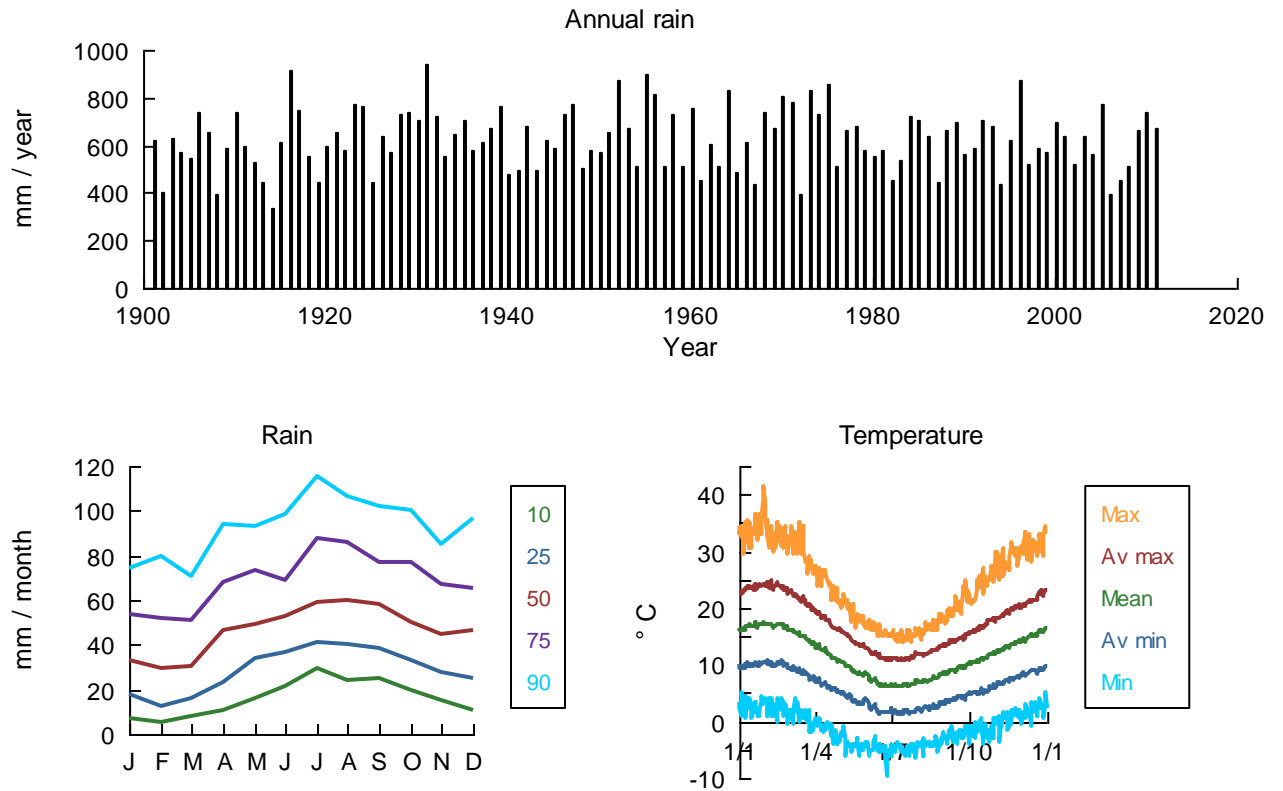
7.3.1 Hamilton Vic



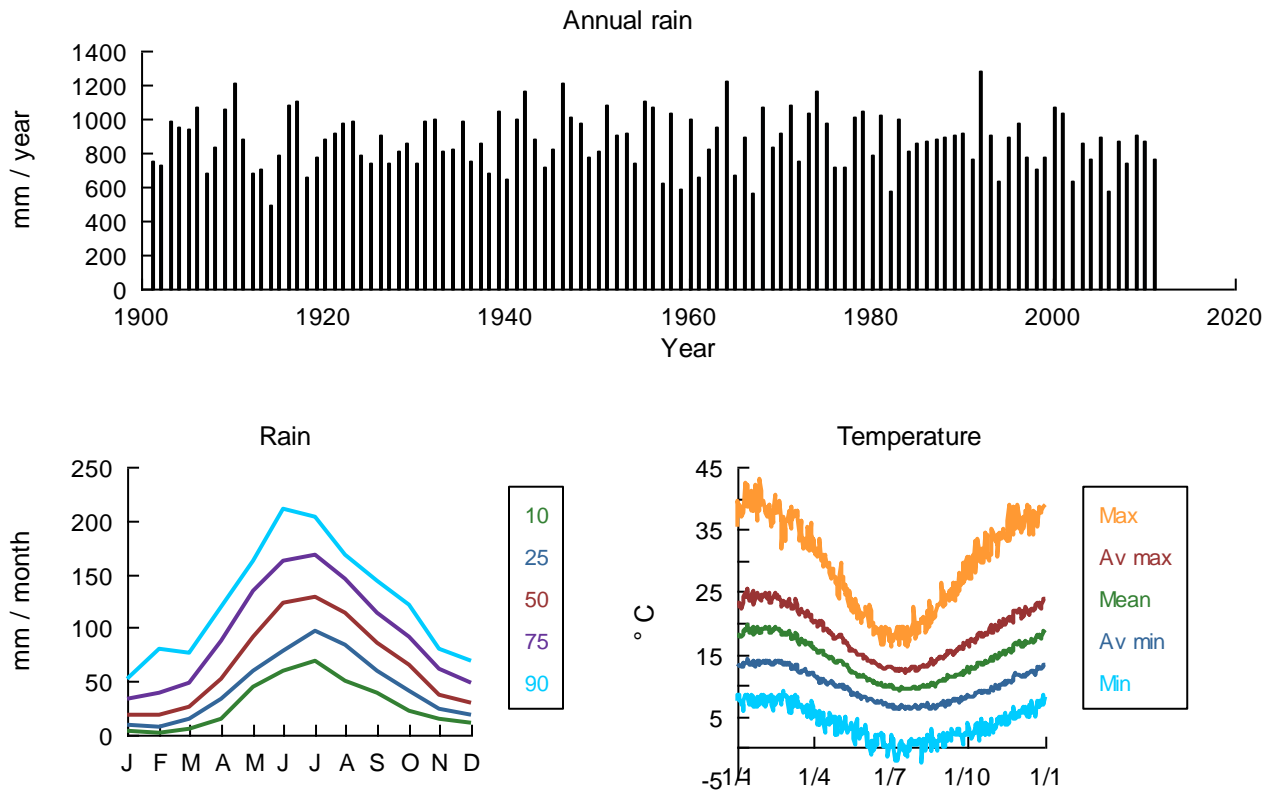
7.3.2 Chiltern, Vic



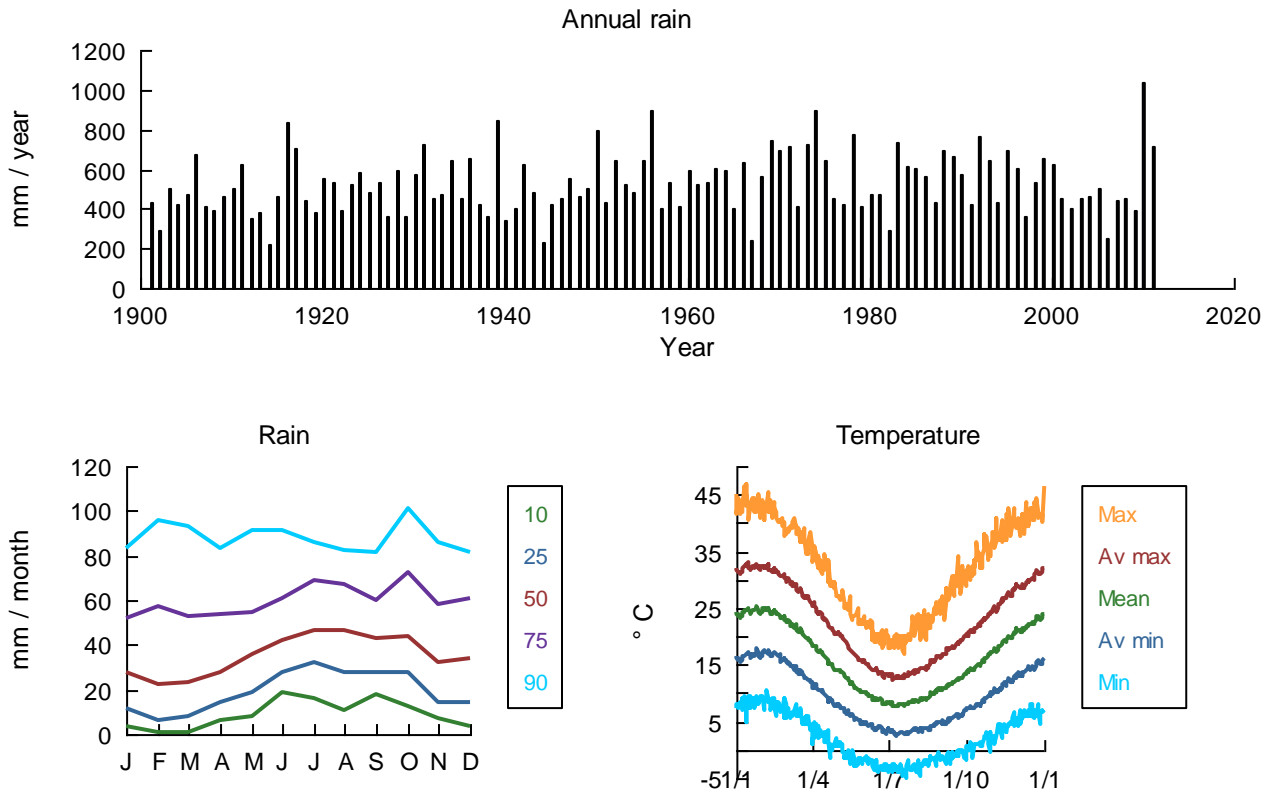
7.3.3 Cressy, Tasmania



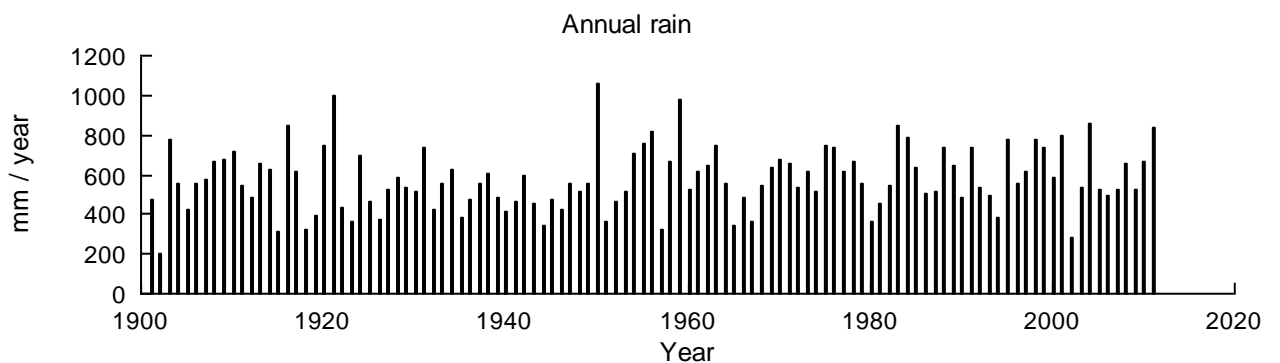
7.3.4 Inman Valley, SA

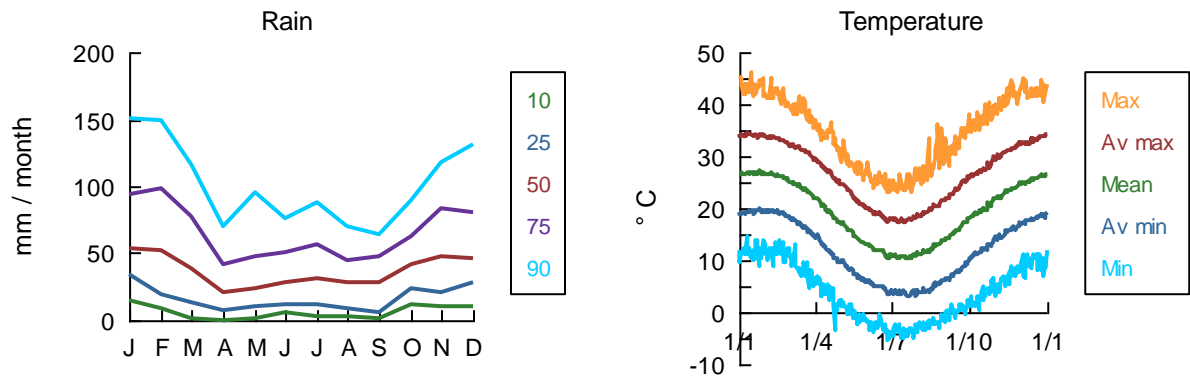


7.3.5 Wagga Wagga, NSW

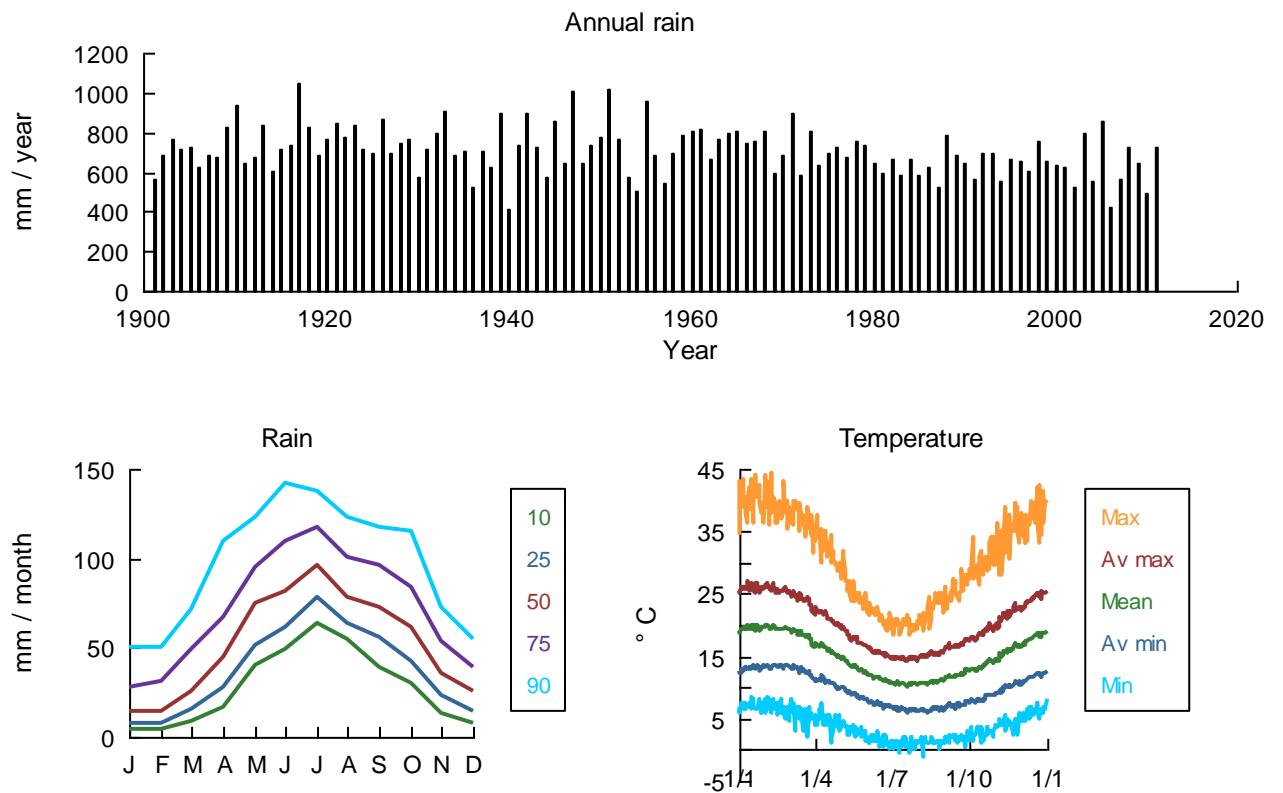


7.3.6 Moree, NSW

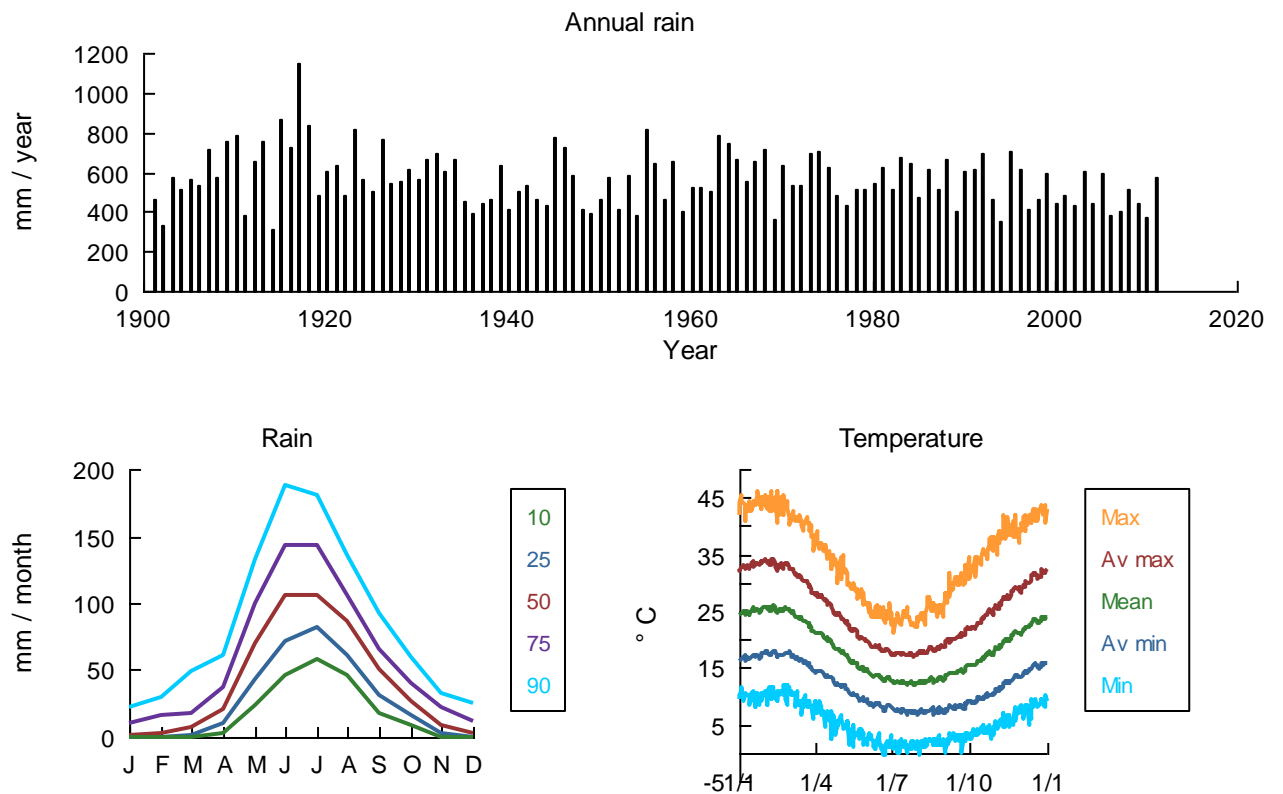




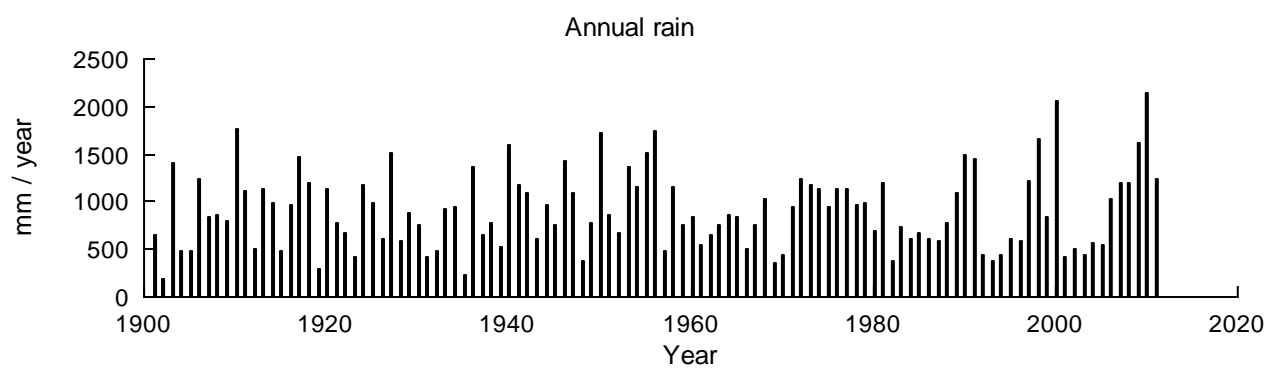
7.3.7 Mt Barker, WA

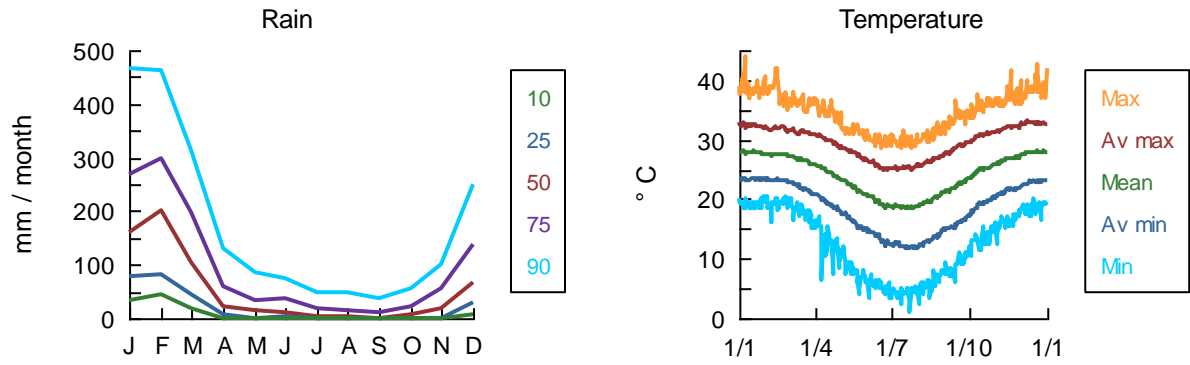


7.3.8 Badgingarra, WA

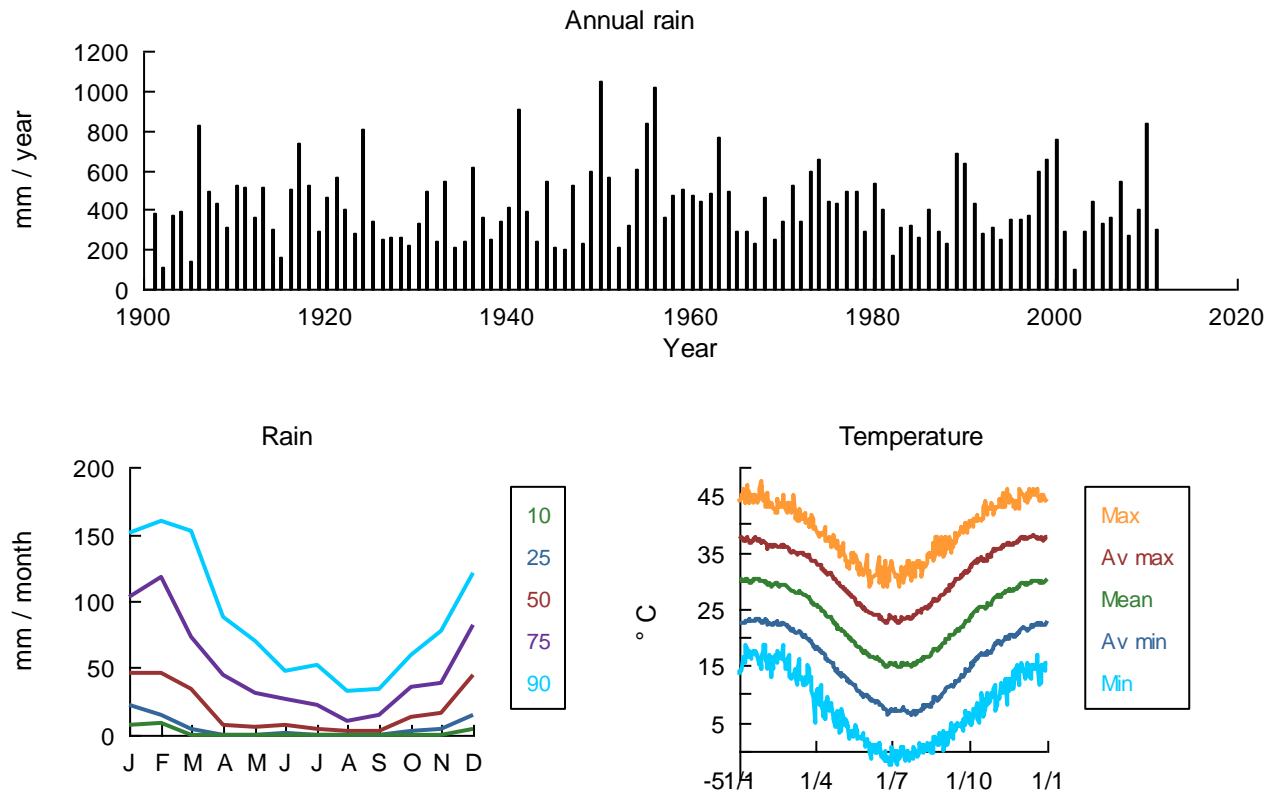


7.3.9 Woodstock, QLD





7.3.10 Longreach, QLD



7.3.11 Kidman Springs, NT

